

# Genome-wide analysis of heart failure yields insights into disease

## heterogeneity and enables prognostic prediction in the Japanese population

**Authors:** Nobuyuki Enzan<sup>1-3</sup>, Kazuo Miyazawa<sup>1</sup>, Satoshi Koyama<sup>1,2,4</sup>, Ryo Kurosawa<sup>1</sup>, Hirotaka Ieki<sup>1,5</sup>, Hiroki Yoshida<sup>1,6</sup>, Fumie Takechi<sup>1,7</sup>, Masashi Fukuyama<sup>1,6</sup>, Ryosuke Osako<sup>1,8</sup>, Kohei Tomizuka<sup>9</sup>, Xiaoxi Liu<sup>9</sup>, Kouichi Ozaki<sup>1,10</sup>, Yoshihiro Onouchi<sup>1,11</sup>, BioBank Japan Project, Koichi Matsuda<sup>12</sup>, Yukihide Momozawa<sup>13</sup>, Hiroyuki Aburatani<sup>14</sup>, Yoichiro Kamatani<sup>15</sup>, Takanori Yamaguchi<sup>8</sup>, Akazawa Hiroshi<sup>6</sup>, Koichi Node<sup>8</sup>, Patrick T. Ellinor<sup>2,3,16</sup>, Michael G. Levin<sup>17,18</sup>, Scott M. Damrauer<sup>18,19</sup>, Benjamin F. Voight<sup>20-22</sup>, Jacob Joseph<sup>23,24</sup>, Yan V. Sun<sup>25,26</sup>, Chikashi Terao<sup>9</sup>, Toshiharu Ninomiya<sup>27</sup>, Issei Komuro<sup>28,29</sup> and Kaoru Ito<sup>1\*</sup>

### Affiliations:

1. Laboratory for Cardiovascular Genomics and Informatics, RIKEN Center for Integrative Medical Sciences, Yokohama, Japan.
2. Cardiovascular Research Center, Massachusetts General Hospital, Boston, MA, USA.
3. Cardiovascular Disease Initiative, The Broad Institute of MIT and Harvard, Cambridge, MA, USA.
4. Program in Medical and Population Genetics, Broad Institute of Harvard and MIT, Cambridge, MA, USA.
5. Department of Genetics, Stanford University School of Medicine, Stanford, USA.
6. Department of Cardiovascular Medicine, Graduate School of Medicine, The University of Tokyo, Tokyo, Japan.

- 23 7. Department of pediatrics Graduate School of Medical and Pharmaceutical Sciences, Chiba  
24 University, Chiba, Japan.
- 25 8. Department of Cardiovascular Medicine, Saga University, Saga, Japan.
- 26 9. Laboratory for Statistical and Translational Genetics, RIKEN Center for Integrative Medical  
27 Sciences, Kanagawa, Japan.
- 28 10. Medical Genome Center, Research Institute, National Center for Geriatrics and Gerontology,  
29 Obu, Japan.
- 30 11. Department of Public Health, Chiba University Graduate School of Medicine, Chiba, Japan.
- 31 12. Laboratory of Clinical Genome Sequencing, Department of Computational Biology and  
32 Medical Sciences, Graduate School of Frontier Sciences, The University of Tokyo, Tokyo,  
33 Japan.
- 34 13. Laboratory for Genotyping Development, RIKEN Center for Integrative Medical Sciences,  
35 Kanagawa, Japan.
- 36 14. Genome Science Division, Research Center for Advanced Science and Technology, The  
37 University of Tokyo, Tokyo, Japan.
- 38 15. Laboratory of Complex Trait Genomics, Department of Computational Biology and Medical  
39 Sciences, Graduate School of Frontier Sciences, The University of Tokyo, Tokyo, Japan.
- 40 16. Demoulas Center for Cardiac Arrhythmias, Massachusetts General Hospital, Boston, MA,  
41 USA.
- 42 17. Division of Cardiovascular Medicine, Perelman School of Medicine, University of  
43 Pennsylvania, Philadelphia, PA, USA.
- 44 18. Corporal Michael J. Crescenz VA Medical Center, Philadelphia, PA, USA.

- 45 19. Department of Surgery, University of Pennsylvania Perelman School of Medicine,  
46 Philadelphia, PA, USA.
- 47 20. Department of Genetics, University of Pennsylvania Perelman School of Medicine,  
48 Philadelphia, PA, USA.
- 49 21. Department of Systems Pharmacology and Translational Therapeutics, University of  
50 Pennsylvania Perelman School of Medicine, Philadelphia, PA, USA.
- 51 22. Institute of Translational Medicine and Therapeutics, University of Pennsylvania Perelman  
52 School of Medicine, Philadelphia, PA, USA.
- 53 23. Veterans Affairs Providence Healthcare System, Providence, RI, USA.
- 54 24. Brown University, Providence, RI, USA.
- 55 25. VA Atlanta Health Care System, Decatur, GA, USA.
- 56 26. Emory University Rollins School of Public Health, Atlanta, GA, USA.
- 57 27. Department of Epidemiology and Public Health, Graduate School of Medical Sciences,  
58 Kyushu University.
- 59 28. Department of Frontier Cardiovascular Science, Graduate School of Medicine, The  
60 University of Tokyo, Tokyo, Japan.
- 61 29. International University of Health and Welfare.  
62
- 63 Correspondence should be addressed to K.I. (kaoru.ito@riken.jp) and I.K. (komuro-  
64 tky@umin.ac.jp )

**Abstract:**

To understand the genetic basis of heart failure (HF) in the Japanese population, we performed genome-wide association studies (GWASs) comprising 16,251 all-cause HF cases, 4,254 HF with reduced ejection fraction cases, 7,154 HF with preserved ejection fraction cases, and 11,122 non-ischemic HF cases among 213,828 individuals and identified five novel loci. A subsequent cross-ancestry meta-analysis and multi-trait analysis of the GWAS data identified 19 novel loci in total. Among these susceptibility loci, a common non-coding variant in *TTN* (rs1484116) was associated with reduced cardiac function and worse long-term mortality. We leveraged the HF meta-GWASs along with cardiac function-related GWASs to develop a polygenic risk score (PRS) for HF. The PRS successfully identified early-onset HF and those with an increased risk of long-term HF mortality. Our results shed light on the shared and distinct genetic basis of HF between Japanese and European populations and improve the clinical value of HF genetics.

## Introduction

Heart failure (HF) is increasing in prevalence and incidence<sup>1</sup>. A previous genome-wide association study (GWAS) of all-cause HF identified 47 risk loci<sup>2</sup>. Considering that GWAS of coronary artery disease (CAD) yielded 175 susceptibility loci<sup>3</sup> and GWAS of atrial fibrillation (AF) yielded 150 loci<sup>4</sup>, the number of loci for HF was lower than expected even when using multi-trait analysis of GWAS (MTAG) that jointly analyzes GWAS summary statistics of multiple related traits, boosting statistical power by leveraging information across traits. This is partly because HF is a heterogeneous syndrome resulting from multiple etiologies. GWAS of HF with reduced ejection fraction (HFrEF) and HF with preserved ejection fraction (HFpEF) was performed to address this heterogeneity<sup>5</sup>. This study identified additional susceptibility loci that had not been found in the all-cause HF GWAS. Given this fact, analysis of HF subtypes should be useful to better understand the genetic architecture for HF. On the other hand, since the vast majority of these HF-GWASs have been performed in European populations, the genetic pathophysiology of HF in non-European populations is not well understood. Additionally, it is difficult to apply polygenic risk scores (PRSs) derived from such GWASs to non-European populations.

Therefore, in the present study, we performed a large-scale Japanese GWAS to explore the genetic architecture of all-cause HF and HF subtypes: HFrEF, HFpEF, and non-ischemic HF (NIHF), followed by a cross-ancestry meta-analysis. Further, we investigated potential causal genes at the identified HF-associated loci by integrating several prioritization methods to characterize the underlying mechanism, clarify the link with cardiomyopathy, and propose gene-drug interactions relevant to HF. We also evaluated the impact of common variants in established cardiomyopathy genes on HF phenotypes and long-term mortality. Subsequently, we

100 identified a *TTN* common variant, which affected HF severity and mortality rate. Additionally,  
101 we developed a PRS derived from the cross-ancestry meta-analysis of each HF subtype along  
102 with HF-related phenotypes and demonstrated the ability of the HF-PRS to predict the early  
103 onset of HF and stratify the long-term mortality, which may provide evidence for the clinical  
104 utility of HF-PRS and lay the foundation for the realization of precision medicine in HF.

## Results

### GWAS revealed a Japanese-specific genetic architecture of HF

An overview of the study design is shown in **Fig. 1**. We performed Japanese case-control GWASs to investigate the association of up to 7,974,473 common genetic variants in the autosomes (minor allele frequency (MAF) > 1%) with the risk of four HF phenotypes. 16,251 HF cases were identified, including 4,254 cases of HFrEF, 7,154 cases of HFpEF, and 11,122 cases of NIHF (**Fig. 1**). Cases of all-cause HF, HFrEF, and HFpEF were compared with 197,577 controls. For the NIHF analysis, CAD cases were excluded from control samples, and 171,995 controls were used. Sample overlaps between each HF phenotype are shown in **Supplementary Fig. 1a**. The mean LV ejection fraction (LVEF) was 48.94% for all-cause HF, 28.74% for HFrEF, 62.08% for HFpEF, and 50.86% for NIHF (**Supplementary Table 1**). These GWASs identified 18 genome-wide significant loci in total, of which five were previously unreported (**Fig. 2a**, **Supplementary Fig. 1b**, **Supplementary Fig. 1c**, **Supplementary Table 2**, and **Supplementary Datasets**). The estimated heritability for each HF phenotype is described in **Supplementary Notes 1**. We assessed the 62 previously reported HF loci and confirmed that their effects were mostly concordant with our Japanese GWAS (**Supplementary Notes 2**, **Supplementary Fig. 2**, **Supplementary Table 3**). Additionally, while the reproducibility of the novel loci was obtained in both internal and external replications, two of the novel loci were specific to the Japanese population and were not found in Europeans (**Supplementary Notes 3**, **Supplementary Fig. 3a, b, c, d** and **Supplementary Table 4, 5**).

To identify HF-associated variants independent of the lead variant at each locus, we performed a stepwise conditional analysis, in which three independent variants (locus-wide  $P < 5.0 \times 10^{-6}$ ) were additionally detected, increasing the total number of HF-associated signals to 21

(**Supplementary Table 6**). Among these, the frequencies of rs893363 (Alternative allele frequency; EAS 96.2% vs. EUR 61.9%,  $\beta = -0.167$  in NIHF) and rs4307025 (Alternative allele frequency; EAS 73.0% vs. EUR 28.0%,  $\beta = 0.0912$  in NIHF) differed significantly between East Asians and Europeans.

To assess the pleiotropic effects, we used the lead variant in each locus as a proxy and assessed its effect sizes in Japanese GWAS of cardiovascular-related phenotypes<sup>6</sup>. The novel variant rs35593046 found in all-cause HF ( $\beta = -0.0630$ ) /NIHF ( $\beta = -0.0767$ ) had a protective role against high blood pressure (**Supplementary Fig. 4a** and **Supplementary Table 7**). It is the intronic variant of *CACNA1D* and is much more frequently observed in the East Asian population than in European populations (53.8% vs. 26.8%).

### **Common variants in cardiomyopathy genes were responsible for HF development**

We then sought to prioritize potential causal genes at the identified HF-associated loci. First, of the 310 variants in LD ( $r^2 > 0.8$ ) with 18 lead variants, 6 missense variants were observed (**Supplementary Table 8**). Among loci previously reported only in the multi-trait analysis of GWAS (MTAG), we found missense variants rs11718898, rs2305398, and rs3732678 in the *CAND2* gene, three of which were in high LD. *CAND2* has been reported to link mTOR signaling to pathological cell growth leading to cardiac remodeling<sup>7</sup>. A missense variant rs2627043 found in the HFrEF GWAS encodes *TTN*, one of the well-known cardiomyopathy genes. Notably, the allele frequency was much higher in the East Asian population than in European populations (64.7% vs. 20.1%). We also found the East Asian-specific missense variant rs671 encoding *ALDH2*, which has been reported to be an HF-related variant in the BBJ 1<sup>st</sup> cohort<sup>6</sup>.



Next, we assessed whether the lead variants we identified were functioning as an expression quantitative trait locus (eQTL) or a splicing quantitative trait locus (sQTL) using GTEx version 8 data. Among the lead variants in novel loci, rs6471480 was found to be an eQTL in subcutaneous adipose tissue (**Supplementary Fig. 4c** and **Supplementary Table 9**) and an sQTL in the left atrial appendage (**Supplementary Fig. 4d** and **Supplementary Table 10**) for the *DPY19L4* gene. Additionally, all of the five HFrEF-related variants, previously identified only in MTAG with cardiac measurements<sup>2</sup>, were revealed as eQTL in the left ventricle. This result may suggest that MTAG in the previous study conferred additional statistical power to discover these variants by integrating cardiac function-related traits.

We conducted gene-based analyses, MAGMA<sup>8</sup> and H-MAGMA<sup>9</sup>, utilizing promoter capture Hi-C in cardiovascular-related tissues<sup>10</sup>. Among novel loci, *DPY19L4* reached statistical significance (FDR < 0.05) in the aorta and adrenal gland using H-MAGMA but not MAGMA (**Supplementary Fig. 4e** and **Supplementary Table 11-12**). Given that the aorta and adrenal gland are known to be involved in the pathophysiology of hypertension, this is consistent with the association of *DPY19L4* with the use of a calcium channel blocker, one of the antihypertensive drugs<sup>6</sup>.

Furthermore, related to the HF loci identified in our Japanese GWAS, we assessed nearby genes containing variants classified in ClinVar as having pathogenic evidence for HF-relevant monogenic disorders, knock-out mouse phenotype, and known cardiomyopathy genes<sup>11</sup>. *NEBL*, located within 500kb of the lead variant rs7075837, was reported to harbor pathogenic variants responsible for primary dilated cardiomyopathy according to the ClinVar database (**Supplementary Table 13**). *NEBL* was also one of the known cardiomyopathy genes (**Supplementary Table 14**), and *Nebl* knock-out mice showed dilatation of the left atrium and

ventricle (**Supplementary Table 15**). *SPRED2* harbors pathogenic variants responsible for Noonan syndrome, which causes hypertrophic cardiomyopathy (**Supplementary Table 13**). Knock-out of *Spred2* also causes dilatation of the heart (**Supplementary Table 15**). Knock-out of *Csmd1* showed obesity and abnormal glucose metabolism (**Supplementary Table 15**). Polygenic Priority Score (PoPS) was recently introduced to estimate responsible genes using various gene features, such as cell-type-specific gene expression and biological pathways. We thus used PoPS to choose the top two likely genes in each locus. As a result, *SPRED2* and *CSMD1* were also prioritized (**Supplementary Table 16**).

Taken together, *DPY19L4*, *CSMD1*, *SPRED2*, and *NEBL* were prioritized by at least three out of 10 predictors as Japanese-specific HF-related genes (**Fig. 2a, 2b**, and **Supplementary Table 17**). Of note, common variants in cardiomyopathy genes *NEBL* were also responsible for HF development. *NEBL* encodes the cardiac Z-disk protein nebulin, and rare variants in this region cause dilated, hypertrophic, and LV non-compaction cardiomyopathy<sup>12</sup>. *DPY19L4* was likely to act on arteries to cause hypertension based on pleiotropic effects and H-MAGMA results. This interpretation was supported by the fact that quercetin, which attenuated atherosclerosis via modulating oxidized LDL-induced endothelial cellular senescence, downregulated *DPY19L4* in human aortic endothelial cells<sup>13</sup>. Based on knockout phenotypes, *CSMD1* is likely to cause HF through metabolic disorders, consistent with a previous study<sup>14</sup>. *SPRED2* loss-of-function induced defects in convergence and extension cell movements leading to cardiac defects and Noonan-like syndrome<sup>15</sup>. Aside from novel loci, *AOPEP*, previously reported in Japanese all-cause HF GWAS<sup>6</sup>, was also associated with HFrEF, HFpEF, and NIHF and the Japanese-specific signal (**Supplementary Fig. 5**). Given that *AOPEP* cleaves

angiotensin III to angiotensin IV, a bioactive peptide of the renin-angiotensin pathway, it is likely that *AOPEP* is responsible for HF development through hypertension.

## Cross-ancestry meta-analysis identified seven novel loci for HF

To improve the statistical power to detect further genetic associations with HF, we conducted cross-ancestry meta-analyses by combining the current Japanese GWAS (BBJ), along with European<sup>2</sup>, Chinese<sup>16</sup>, American<sup>17</sup>, and African<sup>2</sup> all-cause HF GWAS, European HFrEF and HFpEF GWAS<sup>5</sup>, and the UK biobank<sup>18</sup> and FinnGen (data release 9) NIHF GWAS (**Supplementary Table 18** and **Supplementary Notes 4**). These analyses identified 58 HF-associated loci with genome-wide significance ( $P < 5.0 \times 10^{-8}$ ; **Supplementary Fig. 6**, **Supplementary Fig. 7a**, **Supplementary Table 19**, and **Supplementary Datasets**). Of these loci, seven have not been reported previously, including one novel locus detected in the current Japanese GWAS (*CACNA1D* locus). In total, we identified 11 novel loci through the current Japanese GWAS and cross-ancestry meta-analysis.

In internal replication, all the newly identified loci were nominally significant both in East Asian and European populations (**Supplementary Fig. 7b** and **Supplementary Table 20**). rs35593046 (*CACNA1D*), rs7659823 (*EDNRA*), rs5823966 (*ZNF397*), and rs1541596 (*CARM1*) were much more frequently observed in the East Asian population (**Supplementary Fig. 7c** and **Supplementary Table 20**). Replication analyses of three lead variants in HFrEF and HFpEF using independent datasets showed concordant results with the same effect direction (**Supplementary Notes 5**, **Supplementary Figure 7d, e**, and **Supplementary Table 21**).

## Genes related to arrhythmia, metabolism, and heart morphology were prioritized in the cross-ancestry meta-analyses

Of the 1,621 variants in LD ( $r^2 > 0.8$ ) with 75 lead variants in any of the HF subtypes, 10 missense variants and one stop-gain variant were observed (**Supplementary Table 22**). We found an additional missense variant rs2305397 in the *CAND2* gene.

We performed a transcriptome-wide association study (TWAS) and splicing-TWAS using the identified loci in the cross-ancestry meta-analyses and the GTEx data. Among novel loci, *ZNF397* was prioritized in the tibial artery by TWAS (**Supplementary Fig. 8a** and **Supplementary Table 23**). As for loci previously found only in MTAG, *MTSSI*, *PROM1*, and *SPATA24* were prioritized in the left ventricle or left atrial appendage and *CCDC136* was prioritized in the tibial artery. The splicing-TWAS showed that *ZNF397* (left ventricle) and *EDNRA* (left ventricle and left atrial appendage) were prioritized among the novel loci (**Supplementary Fig. 8b** and **Supplementary Table 24**). *TTN*, *SMARCB1*, *SPATA24*, *EFCAB13*, *CCDC136*, *CAND2*, and *CARM1* were prioritized in the left ventricle or left atrial appendage. Gene-based analysis by MAGMA showed that *CACNA1D*, *LHX3*, *EDNRA*, and *ZNF397* reached statistical significance (**Supplementary Fig. 8c** and **Supplementary Table S25** and **S26**).

Among the novel loci, no gene harbored pathogenic variants responsible for cardiovascular-related phenotypes according to the ClinVar database (**Supplementary Table 27**). Based on genetic knockout phenotypes in mice, *Cacna1d* deletion caused arrhythmia (**Supplementary Table 28**) and was prioritized by PoPS (**Supplementary Table 29**). Knockout of *Ednra* showed abnormal heart and aortic morphology (**Supplementary Table 28**) partly

because *Ednra* was associated with heart development<sup>19</sup>. Deletion of *Carm1* caused dilatation of the left atrium, and deletion of *Lhx3* caused decreased body weight (**Supplementary Table 28**).

In the cross-ancestry meta-analyses, *EDNRA*, *ZNF397*, *CACNA1D*, *CARM1*, *LHX3*, and *PDE3A* were prioritized by at least three predictors (**Fig. 2a, 2b**, and **Supplementary Table 30**). Among these six genes, *EDNRA* and *PDE3A* were linked to existing medications (refer to **Candidate drugs linked to disease susceptibility loci** section in the main text). No prioritized gene was found associated with rs10851802 (**Supplementary Notes 6**).

## **The HF-related common variant in the cardiomyopathy gene *MYBPC3* was identified in MTAG**

To further enhance the statistical power of HF GWAS, we conducted MTAG<sup>20</sup>. First, we assessed the genetic correlation between HF and cardiac MRI parameters for the left ventricle<sup>11</sup>, left atrium<sup>21</sup>, right ventricle, right atrium<sup>22</sup>, left ventricular mass<sup>23</sup>, and fibrosis<sup>24</sup>. Because left ventricular mass was strongly correlated with HF in all of the HF subtypes (**Supplementary Fig. 9a and Supplementary Table 31**), we integrated HF GWAS and left ventricular mass GWAS by MTAG. We then found an additional eight novel loci (**Supplementary Fig. 9b, 9c, Supplementary Table 32, and Supplementary Datasets**). Of the 1,597 variants in LD ( $r^2 > 0.8$ ) with 36 lead variants, seven missense variants were observed (**Supplementary Table 33**). Among the novel loci, rs6265 is a missense variant for *BDNF* (**Supplementary Table 33**). TWAS showed that *BDNF* and *ILRUN* were prioritized in the left ventricle and atrial appendage, and *PLPP3* in the fibroblasts (**Supplementary Fig. 10a and Supplementary Table 34**). Splicing-TWAS showed that *ILRUN* (left ventricle and atrial appendage), *BDNF* (coronary artery/aorta/fibroblasts), and *SLC4A7* (fibroblasts) were prioritized (**Supplementary Figure 10b**).

and **Supplementary Table 35**). *SLC4A7*, *MYBPC3*, *BDNF*, and *PCSK1* reached statistical significance in gene-based analyses (**Supplementary Fig. 10c** and **Supplementary Table 36-37**).

Combined with known Mendelian genes (**Supplementary Table 38**), mouse phenotypes (**Supplementary Table 39**), and PoPS (**Supplementary Table 40**), *BDNF*, *MYBPC3*, *SLC4A7*, *ILRUN*, *PCSK1*, *PTPRJ*, and *PLPP3* were prioritized (**Fig. 2a, 2b, Supplementary Table 41**). Notably, common variants in one of the known cardiomyopathy genes *MYBPC3* were responsible for HF development as well as *TTN*, *NEBL* and *BAG3*. Other prioritized genes are described in **Supplementary Notes 7**.

Here, comparing the disease susceptibility loci detected by the Japanese GWAS, European GWAS, cross-ancestry meta-analyses, and MTAG, we found that there were common and different genetic effects between the East Asian and European populations. Among novel loci found in BBJ-specific or cross-ancestry meta-analyses, *AOPEP*, *CSMD1*, *DPY19L4*, and *SPRED2* were significant only in the East Asian population (**Supplementary Fig. 4** and **Supplementary Fig. 11**). On the other hand, *HLA-B*, *APOH*, *CFL2*, *HSD17B12*, *UBA7* were European specific loci (**Supplementary Fig. 11**).

## **Distinct mechanism of each HF phenotype in cross-ancestry analysis**

To compare the mechanisms of each HF phenotype, we conducted a pathway analysis and found that cellular senescence, cyclin-dependent kinase-related pathway, miRNAs involved in DNA damage responses, signaling events mediated by prolactin, Tie2 mediated signaling, and Notch signaling pathway were enriched in all-cause HF (**Fig. 3** and **Supplementary Table 42**). Notch signaling was also enriched in NIHF. From a clinical perspective, miRNAs involved in

DNA damage response may be attractive targets to improve cancer patient outcomes in chemotherapy-related cardiomyopathy, which may be induced by DNA-damaging chemotherapy. The prolactin inhibitor bromocriptine had higher odds of left ventricular function recovery in peripartum cardiomyopathy, one of the leading causes of maternal mortality<sup>25</sup>. Tie2-mediated signaling is not only required for normal vascular development but also is required for ventricular chamber formation<sup>26</sup>. Notch is associated with heart development and regulates cardiac regenerative processes<sup>27</sup>. Aside from cyclin-dependent kinase-related pathways, sarcomere-related pathways including Z-disc, I-band, and actin-binding were enriched in HFrEF (**Fig. 3** and **Supplementary Table 42**). Cardiac cell development/differentiation was enriched in NIHF. On the other hand, no specific pathway was enriched in HFpEF.

Additionally, cell type-specific enrichment analysis with gene expression and epigenetic marks showed that H3K4me1 in the fetal heart was enriched in HFrEF, but the other three HF phenotypes did not show any particular cell type enrichment (**Supplementary Table 43**). Taken together, despite the smaller sample size, HFrEF showed strong enrichment in the heart, especially in the sarcomere.

With miRNA enrichment analysis using MIGWAS, HFrEF showed significant enrichment for the miRNA-target gene network (**Supplementary Figure 12a**). Out of eight candidate miRNA-gene pairs (**Supplementary Table 44**), HSPB7 was also significant in TWAS analysis (**Supplementary Table 34**), suggesting that hsa-mir-4728-*HSPB7* was the most likely pair. *HSPB7* has been reported to be indispensable for heart development and associated with dilated cardiomyopathy<sup>47</sup>.

We conducted the cell type-specific analysis at single-cell resolution using scDRS<sup>48</sup> with healthy, dilated cardiomyopathy, and hypertrophic cardiomyopathy datasets<sup>49</sup>. All four HF

phenotypes showed significant enrichment for cardiomyocytes (**Supplementary Fig 12b** and **Supplementary Table 45**). Additionally, HFpEF showed enrichment for adipocyte and vascular smooth muscle cells<sup>50, 51</sup>, suggesting that HFpEF may have additional mechanisms beyond the other HF phenotypes.

### Candidate drugs linked to disease susceptibility loci

We curated drugs from DrugBank<sup>28</sup> and Therapeutic Target Database<sup>29, 30</sup> (**Supplementary Fig. 13**) for the prioritized genes from the Japanese GWAS, cross-ancestry meta-analyses, and MTAG. Our analysis supports epidemiological evidence that several medications cause or exacerbate HF. Given that knockout of *CACNA1D*, *EDNRA*, and *CDK6* in mice caused abnormal myocardial fiber physiology, abnormal heart ventricle morphology, and decreased myocardial fiber number, respectively, those inhibitors could worsen HF. Indeed, the previous meta-analysis suggested that dihydropyridine calcium channel blockers (nifedipine) can be a risk for HF<sup>31</sup>. The EDNRA inhibitor bosentan caused fluid retention in HF patients<sup>32</sup>. One of the CDK4/6 inhibitors, palbociclib, was associated with worse outcomes in patients who developed atrial fibrillation or HF<sup>33</sup>. All these outcomes were concordant with our genetic analyses.

Tirzepatide, one of the emerging antidiabetics<sup>34, 35</sup>, could be a potential drug repositioning candidate through the *GIPR* locus, which had a protective role against HF. As of now, tirzepatide has not been fully evaluated for its effects on cardiovascular outcomes, but at least it did not increase the risk of cardiovascular events<sup>36</sup>. Currently, a study of tirzepatide in participants with HFpEF (SUMMIT trial) is ongoing (NCT04847557).



## A *TTN* common variant plays an important role in HF outcomes

From the Japanese GWAS and cross-ancestry meta-analyses, we found lead variants associated with cardiomyopathy genes, *TTN*, *NEBL*, and *BAG3* (**Supplementary Table 14**). Given the nature of cardiomyopathy genes, we hypothesized that these variants by themselves could affect cardiac function and prognosis. Among those, the risk allele of *TTN* lead variant (rs1484116) was less frequent in the East Asian populations than in European populations (Risk allele frequency: EUR 0.800, EAS 0.315; **Fig. 4a**) according to the gnomAD database, while we observed the effect size of this variant was higher in Japanese than Europeans (**Fig. 4b**). First, we investigated the association between these variants and cardiac function, and we found that the lead variants of *TTN* (rs1484116) and *BAG3* (rs61870083) were significantly associated with lower left ventricular ejection fraction (*TTN*, effect size -1.16, 95% confidence interval (95%CI) -1.55 - -0.77,  $P = 7.80 \times 10^{-9}$ ; *BAG3*, effect size -2.79, 95%CI -3.58 - -2.00,  $P = 3.88 \times 10^{-12}$ ; **Fig. 4c**). We then repeated the same analysis in NIHF to exclude possible effects of CAD, and it yielded similar results (**Fig. 4c**). These variants of *TTN* and *BAG3* were also associated with lower LVEF in individuals without known cardiac diseases in UKBB cohorts (**Fig. 4c** right panel). Furthermore, we assessed the effects of these common variants on long-term HF mortality among non-HF subjects and HF subjects. The Kaplan-Meier estimates and Cox regression analysis demonstrated that the *TTN* lead variant (rs1484116) was significantly associated with worse outcomes in HF patients (HR 1.24, 95%CI 1.06-1.46,  $P = 8.12 \times 10^{-3}$ ; **Fig. 4d and e**). These results suggest the importance of the *TTN* common variant in risk stratification of HF patients and this variant could be a novel potential biomarker for HF.

## Development of a HF-PRS and its performance

Although most GWASs have been conducted in European populations, PRSs derived from European GWASs have shown poorer performance in other populations. On the other hand, PRSs derived from cross-ancestry GWASs have been reported to improve their accuracy in understudied populations<sup>3</sup>. Furthermore, integrating not only cross-ancestry GWAS of interest but also related phenotypes (e.g., blood pressure and LDL cholesterol for CAD) has proved to enhance the PRS performance<sup>37</sup>. Here, we split our case-control samples into the derivation dataset, dataset for linear combination, test dataset, and survival analysis dataset to avoid sample overlap (**Supplementary Fig. 14**). We derived each PRS from the Japanese all-cause HF, European/American/African all-cause HF, and European HFrEF, HFpEF, CAD, AF, and left ventricular mass with PRS-CS (see Methods section). The linear combination of these PRS was performed by Lasso regression with 10-fold cross-validation, resulting in the exclusion of PRSs calculated from Native American all-cause HF, and European NIHF. For the PRS derived from a single population GWAS, as concordant with the population specificity, the PRS derived from BBJ showed higher performance in the Japanese population than those from European (pseudo  $R^2 = 0.709$  in European versus 0.737 in BBJ; **Fig. 5a**) despite the smaller sample size. As suggested previously, cross-ancestry PRS showed higher performance than those from single population-derived PRS (**Fig. 5a** and **Supplementary Fig. 15a**). Additionally, combining HF-related phenotypes further improved the performance (**Fig. 5a** and **Supplementary Fig. 15a**). Hereafter, we used the best model (model J in **Fig. 5a**). The risk of developing HF in individuals with top PRS quintile was two times higher than that with bottom quintile (pseudo  $R^2$  with 95% CI for bottom quintile, 0.095 [0.084-0.107]; top quintile, 0.198 [0.183-0.214]; **Supplementary Fig. 15b**).

## Impact of HF-PRS on HF phenotypes and outcomes

The impact of HF-PRS on long-term outcomes has not been previously evaluated. Earlier all-cause HF GWAS<sup>2</sup> and HFrEF/HFpEF GWAS<sup>5</sup> did not develop a PRS. Although the Global Biobank Meta-analysis Initiative (GBMI) developed an HF-PRS, it only assessed the predictive performance and not the clinical impact<sup>38</sup>. To assess the potential of the HF-PRS for clinical applications, we investigated the association between the PRS and the onset age of HF in individuals from our BBJ case samples (n=10,810). We observed that the onset age decreased as the PRS increased; individuals with the top tertile PRS were estimated to be approximately two years younger at HF onset compared to the bottom tertile individuals (**Fig. 5b**). To further explore the clinical utility of the HF-PRS, we assessed its impact on mortality using long-term follow-up data in BBJ. We stratified individuals without HF by tertiles (low, intermediate, and high groups) based on their PRS scores. The Kaplan–Meier estimates of cumulative cardiovascular mortality rate were significantly increased in the high PRS group. Furthermore, we demonstrated that the HF-PRS successfully stratified the risk of HF death (**Fig. 5c**).

## Discussion

We performed a large-scale GWAS with 16,251 HF cases and subtypes in the Japanese population along with cross-ancestry meta-GWAS and MTAG boosted by heart function-related traits and identified 19 novel loci. Additionally, through various gene prioritization approaches, we elucidated associations with clinical risk factors, cardiomyopathy, and drug targets. Furthermore, analysis of various datatypes in the biobank, including clinical and long-term prognosis data from biobanks, confirmed the identification of significant HF variants and the clinical utility of HF-PRS described here.

The Japanese GWAS identified 20 genome-wide significant loci associated with HF. This includes five new loci, where variants significantly prevalent in East Asians. We identified a novel association in the *CACNAID* loci, suggesting the involvement of functional alterations in the calcium voltage-gated channel as a mechanism underlying HF. Since *CACNAID* encodes the pore-forming  $\alpha 1$  subunit of  $\text{Ca}_v1.3$  voltage-gated L-type calcium channels (LTCC) and is highly expressed in the sinus node and atrioventricular nodes<sup>39</sup>. Mutations in *CACNAID* have been proved to cause sinoatrial node dysfunction<sup>40</sup> suggesting the contribution of *CACNAID* in the development of HF through chronotropic incompetence.

Furthermore, we performed cross-ancestry meta-analyses for HF subtypes, where 58 genome-wide significant loci were identified, resulting in the discovery of eight new loci. Among the prioritized genes based on the GWAS, *EDNRA*, and *CACNAID* had a protective role against heart failure and are drug targets for other diseases. Both *EDNRA* inhibitors and *CACNAID* inhibitors have already been reported to exacerbate HF, an observation that was successfully supported by our genetic analysis. We also identified a GIP/GLP-1-agonist as a drug

repositioning candidate. By contrast, we genetically proved the detrimental effects of PDE3A and CDK4/6 blockade on HF pathogenesis.

In these analyses, we found that common variants of the cardiomyopathy genes *TTN*, *NEBL*, and *BAG3* contributed to the development of HF. MTAG additionally identified that common variants of *MYBPC3* were one of the susceptibility loci. Among these, a *TTN* common variant rs1484116 had a significant difference in the frequency and effect between Japanese and European populations. Notably, this common variant stratified individuals who went on to develop HF into those with a high mortality rate. Additionally, while rare truncating variants in the *TTN* gene comprise the most common genetic subtype of dilated cardiomyopathy, accounting for up to 25% of cases<sup>41</sup>, we show for the first time that the *TTN* common variant in a non-coding region also causes HF.

Integrating cross-ancestry GWAS of interest and GWAS of related phenotypes improves predictive performance in CAD<sup>37</sup>. In our HF-PRS, integrating HFrEF, HFpEF, AF, CAD, and left ventricular mass improved the performance. Moreover, we demonstrated that HF-PRS could predict HF death in subjects who had not yet been diagnosed as having HF.

Our study has several limitations. First, we did not have other large cohorts for the replication analysis. We did not replicate Japanese-specific HF loci using other East Asian cohorts since there were no other large East Asian biobanks available with enough of these patients. Instead, we assessed these variants with European data, showing the same effect direction. As for cross-ancestry meta-analyses, we did not have a non-overlapping corresponding cohort for all-cause HF and NIHF. Hence, we used European all-cause HF data for the replication of HFrEF and HFpEF cross-ancestry meta-analyses, showing almost the same effect direction. Second, we did not perform quantitative trait-based enrichment analysis (e.g. TWAS

and splicing-TWAS) for the Japanese GWAS since there is no available molecular QTL dataset for the East Asian population. Thus, eQTL, sQTL, and other QTL datasets of the East Asian population are required in future research to further clarify the genetic differences between the East Asian and European populations.

In conclusion, our large-scale Japanese and cross-ancestry genetic analyses identified 19 new risk loci and provided insights into the distinct and shared genetic architecture of HF between Japanese and Europeans. Multiple prioritization methods allowed us to identify candidate genes involved in the pathogenesis. We also showed that the common variant of *TTN* can be a prognostic marker for HF patients in the Japanese population. Furthermore, analyses of disease prediction and long-term survival demonstrated the clinical utility of our HF-PRS. These data highlight the utility of HF genetics in clinical settings and provide useful evidence for the implementation of genomic medicine.

## Online Methods

### Study populations

We included two cohorts for the Japanese-specific meta-analysis including the BBJ 1<sup>st</sup> cohort and BBJ 2<sup>nd</sup> cohort from the BioBank Japan Project<sup>42</sup>. Further details on each cohort are described in the **Supplementary Note**.

For GWAS quality control, we excluded samples with a call rate  $< 0.98$  and related individuals with  $\pi\text{-hat} > 0.2$ , which is an index of relatedness based on pairwise identity-by-descent implemented in PLINK 2.0 (20 Aug 2018 ver.). We then excluded samples with a heterozygosity rate  $> +4$  s.d. We performed principal component analysis (PCA) using PLINK 2.0. and excluded outliers from the Japanese cluster. For the case samples in GWAS, we selected individuals with HF diagnosed by a physician based on accepted medical practice criteria. HFrEF was defined as having HF and LVEF  $< 40\%$ , while HFpEF was defined as having HF and LVEF  $> 50\%$ . NIHF was defined as having HF without CAD. The demographic features of the case-control cohort are shown in **Supplementary Table 1**.

### Genotyping, imputation, and quality control

To construct a population-specific reference panel, we included 7,825 Japanese WGS samples. Each sample was aligned to the human genome assembly GRCh38 and subjected to variant calling individually using the Illumina DRAGEN Bio-IT Platform (versions 3.4.12 and 3.5.7), generating gVCF files. Joint variant calling was subsequently performed with DRAGEN (version 3.6.3), employing default parameters and filtering criteria. Next variant quality control (QC) was conducted and variants from the jointly-called dataset were filtered out based on several exclusion criteria: 1) the presence of multi-alleles; 2) singleton; 3) missing data rate  $>$

5%; 4) Hardy-Weinberg Equilibrium (HWE)  $p$ -value  $< 1 \times 10^{-6}$ . After QC, VCF files were phased on a whole-chromosome basis using SHAPEIT4 (version 4.2)<sup>43</sup>.

GWAS subjects were genotyped using the Illumina Human OmniExpress Genotyping BeadChip or a combination of Illumina HumanOmniExpress and HumanExome BeadChips (Illumina, San Diego, CA). For genotype quality control (QC), we excluded variants with (i) SNP call rate  $< 0.99$ , (ii) MAF  $< 0.01$ , and (iii) Hardy-Weinberg equilibrium  $P$  value  $< 1.0 \times 10^{-6}$ . BBJ 1<sup>st</sup> and BBJ 2<sup>nd</sup> cohorts were separately phased using SHAPEIT2 (version r837) and EAGLE2 (version 2.39), respectively. Imputation was then carried out with Minimac4 (version 1.0.0)<sup>44</sup> with a minor adjustment: variant positions in the array data, initially based on hg19, were remapped to GRCh38 using BLAST based on the sequence of flanking sites.

## GWAS

In the Japanese GWAS, association was performed by logistic regression analysis assuming an additive model with adjustment for age, age<sup>2</sup>, sex, and top 10 principal components (PCs) using REGENIE<sup>45</sup>. We selected variants with Minimac4 imputation quality score of  $> 0.3$  and MAF  $\geq 0.01$ . The genome-wide significance threshold was defined at  $P < 5.0 \times 10^{-8}$ . The genomic inflation factor ( $\lambda_{GC}$ ) was 1.044, 1.080, 1.050, and 1.083 for all-cause HF, HFrEF, HFpEF, and NIHF, respectively. (**Supplementary Figure. 2a**). Adjacent genome-wide significant SNPs were grouped into one locus if they were within 1 Mb of each other. We defined a locus as follows: (1) extracted genome-wide significant variants ( $P < 5.0 \times 10^{-8}$ ) from the association result, (2) added 500 kb to both sides of these variants, and (3) merged overlapping regions. If the locus did not contain coordinates with previously reported genome-wide significant variants (i.e., all variants with  $P < 5.0 \times 10^{-8}$  in the previously reported locus),



the region was annotated as being novel. To identify independent association signals in the loci, we conducted a stepwise conditional analysis for genome-wide significant loci defined as described in the GWAS. First, we performed logistic regression conditioning on the lead variants of each locus. We set a locus-wide significance at  $P < 5.0 \times 10^{-6}$  and repeated this procedure until none of the variants reached locus-wide significance for each locus.

### **Linkage-disequilibrium score regression and heritability**

To estimate confounding biases such as cryptic relatedness and population stratification, we performed a linkage-disequilibrium score regression (LDSC) (Version 1.0.0). We selected SNPs with  $MAF \geq 0.01$  and variants within the major histocompatibility complex region were excluded. For the regression, we used the East Asian LD scores provided by the authors (<https://github.com/bulik/ldsc/>). The all-cause HF population prevalence was set at 6.5% according to the Japan Medical Data Center and the Medical Data Vision datasets<sup>46</sup>. Since 37.4%, 45.1%, and 26.6% of all-cause HF were HFrEF, HFpEF, and NIHF, we assumed population prevalence was 2.4% for HFrEF, 2.9% for HFpEF, and 1.7% for NIHF<sup>47</sup>.

### **Cross-ancestry meta-analysis**

All genomic coordinates were converted to GRCh37 with the liftover tool. Fixed-effect meta-analyses based on inverse-variance weighting were performed for all HF phenotypes. We defined genome-wide significant loci by iteratively spanning the  $\pm 500$  kb region around the most significant variant and merging overlapping regions until no genome-wide significant variants were detected within  $\pm 1$  Mb. A locus was categorized as “known” if the region after merging was within  $\pm 500$  kb of variants for the corresponding phenotype in previous all-cause HF,

HFrEF, HFpEF, NIHF GWAS, “previously reported only in MTAG” if in previous all-cause HF MTAG results<sup>2</sup>, otherwise, it was categorized as a novel. The most significant variant in each locus was selected as the index variant. Cochran’s Q-test for heterogeneity was conducted to identify loci with index variants that have different effect sizes across GWAS data sets. We filtered variants with strong heterogeneity ( $P_{het} < 1.0 \times 10^{-4}$ ) or MAF < 1%.

### Multi-trait association study

To identify additional HF-risk loci, we used MTAG<sup>20</sup> in Europeans, including cardiac MRI traits, which were most strongly correlated with HF. We included left ventricular mass as it was most strongly correlated with all HF phenotypes (**Supplementary Figure 9a**). We filtered variants with MAF < 1% and defined genome-wide significant loci in the same way as trans-ancestry meta-analysis.

### Independent follow-up of GWAS signals

We sought to replicate internally the HF-risk loci reaching genome-wide significance in the Japanese GWAS meta-analyses within BBJ1 and BBJ2. As for genome-wide significant variants identified in the cross-ancestry meta-analysis, we assessed EUR and EAS. As external replication of associations, we assessed significant variants identified in HFrEF or HFpEF using European all-cause HF.

### Genetic correlation of HF and cardiac imaging traits

Cross-trait LDSC was performed to estimate genetic correlation ( $r_g$ ) between HF and cardiac MRI traits. LDSC is a computationally efficient method that utilizes GWAS summary

statistics to estimate heritability and genetic correlation between polygenic traits while accounting for sample overlap.

## Transcriptome-wide association study

We performed a transcriptome-wide association study (TWAS) to assess gene-HF associations using FUSION<sup>48</sup>, which estimates the association between predicted gene expression levels and a phenotype of interest using summary statistics and gene expression prediction models. We used precomputed prediction models of gene expression in tissues considered to be relevant for HF with LD reference data in GTEx v8 and the summary statistics of the trans-ancestry HF-GWAS as input. Furthermore, we used the cross-tissue weights generated in GTEx v8 using sparse canonical correlation analysis (sCCA) across 49 tissues available on the FUSION website, including gene expression models for the first three canonical vectors (sCCA1-3), which were shown to capture most of the gene expression signal. Transcriptome-wide significant genes (eGenes) and the corresponding eQTLs were determined using the Bonferroni correction, based on the average number of features (8,036.5 genes) tested across all reference panels and correcting for the four HF phenotypes ( $P < 1.55 \times 10^{-6}$ ). To ensure that the observed associations did not reflect a random correlation between gene expression and non-causal variants associated with stroke, we performed a colocalization analysis on the eGenes to estimate the posterior probability of a shared causal variant between the gene expression and trait association (PP4). eGenes presenting a  $PP4 \geq 0.75$  were considered to be significant.

## Splicing-TWAS

We performed a splicing-TWAS to assess splicing-HF associations using MetaXcan. We used GTEx v8 MASHR-based models (<https://github.com/hakyimlab/MetaXcan>). The significant splicing sites were determined using the Bonferroni correction, based on the number of splicing sites multiplied by the four HF phenotypes.

## Identifying protein-altering variants

To identify protein-altering variants among our genome-wide significant associations, we took the sentinel variants and their LD proxies at  $r^2 \geq 0.8$  as estimated in the European ancestry subset of 1000 Genomes Project phase 3 and annotated them using the Ensembl VEP. We selected for each sentinel variant any proxies identified as having a ‘high’ (that is, stop-gain and stop-loss, frameshift insertion and deletion, donor and acceptor splice-site and initiator codon variants) or ‘moderate’ (that is, missense, in-frame insertion and deletion, splice region) consequence and recorded the gene that the variant disrupts.

## Polygenic prioritization of candidate causal genes

We implemented PoPS, a similarity-based gene prioritization method designed to leverage the full genome-wide signal to nominate causal genes independent of methods utilizing GWAS data proximal to the gene (<https://github.com/FinucaneLab/pops.git>). Broadly, PoPS leverages polygenic enrichments of gene features including cell-type-specific gene expression, curated biological pathways, and protein-protein interaction networks to train a linear model to compute a PoPS for each gene.

## Variants responsible for cardiovascular-relevant monogenic disorders

To identify genes harboring pathogenic variants responsible for HF-relevant monogenic disorders, we searched the NCBI's ClinVar database (<https://www.ncbi.nlm.nih.gov/clinvar/>). Variants were pruned to those within  $\pm 500$  kb of our HF sentinel variants; categorized as 'pathogenic' or 'likely pathogenic'; with a listed phenotype; and with either (i) details of the evidence for pathogenicity, (ii) expert review of the gene or (iii) a gene that appears in practice guidelines<sup>49</sup>. We then filtered the variants that were annotated with a manually curated set of cardiovascular-relevant phenotype terms, including those related to HF and HF risk factors (**Supplementary Tables 12, 24, and 35**). Where a variant was annotated with multiple genes, both genes were considered as potentially pathogenic.

## Phenotyping knock-out mice

Human gene symbols were mapped to gene identifiers (HGNC) and mouse ortholog genes were obtained using Ensembl ([www.ensembl.org](http://www.ensembl.org)). Phenotype data for single-gene knock-out models were obtained from the International Mouse Phenotyping Consortium, data release 19.1 ([www.mousephenotype.org](http://www.mousephenotype.org)), and from the Mouse Genome Informatics database, data from July 2023 ([www.informatics.jax.org](http://www.informatics.jax.org)). For each mouse model, reported phenotypes were grouped using the mammalian phenotype ontology hierarchy into broad categories relevant to HF as follows: abnormal glucose homeostasis (MP:0002078), abnormal blood coagulation (MP:0002551), muscle phenotype (MP:0005369), abnormal lipoprotein level (MP:0010329), abnormal catecholamine level (MP:0011479), abnormal myofibroblast differentiation (MP:0012196), cardiac edema (MP:0012270), abnormal lipid metabolism (MP:0013245), adipose tissue necrosis (MP:0013249), abnormal susceptibility to non-insulin-dependent diabetes (MP:0020086), abnormal fibroblast physiology (MP:0020414), abnormal adipose tissue

noradrenaline turnover (MP:0021021), cardiac amyloidosis (MP:0021148) along with phenotypes previously used in CAD analysis<sup>49</sup> (**Supplementary Table 46**). This resulted in mapping from genes to phenotypes in animals (**Supplementary Tables 14, 25, and 36**).

## **PRS derivation and performance**

First, we divided our dataset into three groups: (i) a discovery group to derive PRS (12,335 cases and 107,333 controls), (ii) a group used for linear combination (1,837 cases and 11,320 controls), (iii) a test group to assess PRS performance (1,837 cases and 11,319 controls), and (iv) a group for the survival analysis (67,991 controls) (**Supplementary Fig. 14**). Next, we used PRS-CS to derive each PRS from Japanese-, European-, American-, African- all-cause HF, European HFrEF, HFpEF, NIHF, AF, CAD, and left ventricular mass. We used LD reference panels constructed using the 1000 Genomes Project phase 3 samples according to each cohort population. Subsequently, we calculated PRSs in the withheld BBJ cohorts for linear combination and conducted logistic regression with L1 regularization and 10-fold cross-validation. Finally, we used the Japanese all-cause HF, European all-cause HF, European HFrEF, European HFpEF, European CAD, European AF, and European left ventricular mass to construct the HF-PRS. The performance of the PRS was measured as (1) Nagelkerke's pseudo- $R^2$  obtained by modeling age, sex, the top 10 PCs, and normalized PRS and (2) the area under the curve of the receiver operator curve in the same model as Nagelkerke's pseudo  $R^2$ . Using the models previously described, we calculated the PRSs and assessed their performance for the independent test cohort.

## **Association of HF-PRS with age of HF onset**

To assess the association between HF-PRS and age at HF onset, we extracted HF case samples with available data on age at HF onset ( $n = 10,810$ , the median age of HF onset was 68 years of age [IQR 60–76]) and constructed a linear regression model of age at HF onset including HF PRS along with sex and the top 10 PCs to estimate effects of HF-PRS on age of AF onset.

### Survival analysis

For survival analysis, the Cox proportional hazards model was used to assess the association between HF-PRS and long-term mortality. We obtained survival follow-up data with the ICD-10 code for 132,737 individuals from the BBJ dataset<sup>42</sup>. The causes of death were classified into three categories according to ICD-10 codes: cardiovascular death (I00–I99) and HF death (I50). For HF-PRS analysis, we used a holdout survival analysis cohort (**Supplementary Figure 10**). The median follow-up period was 8.4 years (IQR 6.8 – 9.9). The Cox proportional hazards model was adjusted for sex, age, the top 10 PCs, and disease status. Analyses were performed with the R package survival v.2.44, and survival curves were estimated using the R package survminer v.0.4.6, with modifications.

## **Data availability**

Summary statistics of Japanese GWAS and polygenic risk scores derived in this study will be publicly available at the National Bioscience Database Center (<https://humandbs.dbcls.jp/en/>). The GWAS summary statistics for HF (GBMI American: <https://www.globalbiobankmeta.org/>; Kadoorie: <https://www.ckbiobank.org/>; FinnGen NIHF: [https://console.cloud.google.com/storage/browser/\\_details/finngen-public-data-r9/summary\\_stats/](https://console.cloud.google.com/storage/browser/_details/finngen-public-data-r9/summary_stats/), R9\_I9\_NONISCHCARDMYOP; UKBB NIHF: <https://cvd.hugeamp.org/>), and cardiac MRI (left ventricle, right ventricle and atrium: <http://kp4cd.org/datasets/mi>; left atrium: <https://zenodo.org/records/5074929>; left ventricular mass: <https://cvd.hugeamp.org/>) traits are publicly available.

## **Code Availability**

The code used in this study is available on reasonable request to the corresponding authors.

## **Acknowledgements**

We thank the staff of BBJ for their assistance in collecting samples and clinical information. We thank Naoko Miyagawa, Akio Wada, and Shuji Ito for their technical assistance. This research was funded by the Japan Agency for Medical Research and Development (AMED) (JP24bm1423005 to K.I, nos. JP24ek0210164, JP24tm0524004, and JP24tm0624002 to K.I., S.N., and I.K., and nos. JP24km0405209 and JP20ek0109487 to K. Miyazawa, K. I., S. K., S. N., H. Akazawa, and I. K.), Japan Foundation for Applied Enzymology (to N.E), the Japan Society for the Promotion of Science (to N. E. and K. I.), and the Research Funding for Longevity Sciences from NCGG (24–15 to K.O. and K.I.). BBJ was supported by



the Tailor-Made Medical Treatment Program of the Ministry of Education, Culture, Sports, Science, and Technology (MEXT) and AMED under grant numbers JP17km0305002, JP17km0305001, and JP24tm0624002.

# **Author Contributions**

N. E., K. I., C. T., Y. K., T. N., and I. K. conceived and designed the study. K. I, C. T., K. Matsuda., Y. M., and Y. K. collected and managed the BBJ sample. T. N, Y. M., and Y. K. performed the genotyping. N. E, K. Miyazawa, S. K, H. I., R.K., H.Y., F.T., M.F., R.O. performed the statistical analyses. N.E, K. I, C. T, S. K., K.T., X.L, K.O., Y. O., T.Y., Y. K., T.N., K.N., H. Akazawa, P.T.E., MG.L., SM.D., BF.V, J.J., and YV.S. contributed to data collection, processing, analysis, and interpretation. K. I, C.T., Y K., H. Aburatani, P.T.E. and I.K. supervised the study. N.E. and K.I. wrote the manuscript, and many authors have provided valuable edits.

# **Competing interests**

The authors declare no competing interests associated with this manuscript.

## References:

1. Ponikowski P, Anker SD, AlHabib KF, Cowie MR, Force TL, Hu S, Jaarsma T, Krum H, Rastogi V, Rohde LE, Samal UC, Shimokawa H, Budi Siswanto B, Sliwa K and Filippatos G. Heart failure: preventing disease and death worldwide. *ESC Heart Fail.* 2014;1:4-25.
2. Levin MG, Tsao NL, Singhal P, Liu C, Vy HMT, Paranjpe I, Backman JD, Bellomo TR, Bone WP, Biddinger KJ, Hui Q, Dikilitas O, Satterfield BA, Yang Y, Morley MP, Bradford Y, Burke M, Reza N, Charest B, Regeneron Genetics C, Judy RL, Puckelwartz MJ, Hakonarson H, Khan A, Kottyan LC, Kullo I, Luo Y, McNally EM, Rasmussen-Torvik LJ, Day SM, Do R, Phillips LS, Ellinor PT, Nadkarni GN, Ritchie MD, Arany Z, Cappola TP, Margulies KB, Aragam KG, Haggerty CM, Joseph J, Sun YV, Voight BF and Damrauer SM. Genome-wide association and multi-trait analyses characterize the common genetic architecture of heart failure. *Nat Commun.* 2022;13:6914.
3. Koyama S, Ito K, Terao C, Akiyama M, Horikoshi M, Momozawa Y, Matsunaga H, Ieki H, Ozaki K, Onouchi Y, Takahashi A, Nomura S, Morita H, Akazawa H, Kim C, Seo JS, Higasa K, Iwasaki M, Yamaji T, Sawada N, Tsugane S, Koyama T, Ikezaki H, Takashima N, Tanaka K, Arisawa K, Kuriki K, Naito M, Wakai K, Suna S, Sakata Y, Sato H, Hori M, Sakata Y, Matsuda K, Murakami Y, Aburatani H, Kubo M, Matsuda F, Kamatani Y and Komuro I. Population-specific and trans-ancestry genome-wide analyses identify distinct and shared genetic risk loci for coronary artery disease. *Nat Genet.* 2020;52:1169-1177.
4. Miyazawa K, Ito K, Ito M, Zou Z, Kubota M, Nomura S, Matsunaga H, Koyama S, Ieki H, Akiyama M, Koike Y, Kurosawa R, Yoshida H, Ozaki K, Onouchi Y, BioBank Japan P, Takahashi A, Matsuda K, Murakami Y, Aburatani H, Kubo M, Momozawa Y, Terao C, Oki S, Akazawa H, Kamatani Y and Komuro I. Cross-ancestry genome-wide analysis of atrial

714   fibrillation unveils disease biology and enables cardioembolic risk prediction. *Nat Genet.*  
715   2023;55:187-197.

716   5.       Joseph J, Liu C, Hui Q, Aragam K, Wang Z, Charest B, Huffman JE, Keaton JM,  
717   Edwards TL, Demissie S, Djousse L, Casas JP, Gaziano JM, Cho K, Wilson PWF, Phillips LS,  
718   Program VAMV, O'Donnell CJ and Sun YV. Genetic architecture of heart failure with preserved  
719   versus reduced ejection fraction. *Nat Commun.* 2022;13:7753.

720   6.       Sakaue S, Kanai M, Tanigawa Y, Karjalainen J, Kurki M, Koshihara S, Narita A, Konuma  
721   T, Yamamoto K, Akiyama M, Ishigaki K, Suzuki A, Suzuki K, Obara W, Yamaji K, Takahashi  
722   K, Asai S, Takahashi Y, Suzuki T, Shinozaki N, Yamaguchi H, Minami S, Murayama S,  
723   Yoshimori K, Nagayama S, Obata D, Higashiyama M, Masumoto A, Koretsune Y, FinnGen, Ito  
724   K, Terao C, Yamauchi T, Komuro I, Kadowaki T, Tamiya G, Yamamoto M, Nakamura Y, Kubo  
725   M, Murakami Y, Yamamoto K, Kamatani Y, Palotie A, Rivas MA, Daly MJ, Matsuda K and  
726   Okada Y. A cross-population atlas of genetic associations for 220 human phenotypes. *Nat Genet.*  
727   2021;53:1415-1424.

728   7.       Gorska AA, Sandmann C, Riechert E, Hofmann C, Malovrh E, Varma E, Kmietczyk V,  
729   Olschlager J, Jurgensen L, Kamuf-Schenk V, Stroh C, Furkel J, Konstandin MH, Sticht C,  
730   Boileau E, Dieterich C, Frey N, Katus HA, Doroudgar S and Volkers M. Muscle-specific Cand2  
731   is translationally upregulated by mTORC1 and promotes adverse cardiac remodeling. *EMBO*  
732   *Rep.* 2021;22:e52170.

733   8.       de Leeuw CA, Mooij JM, Heskes T and Posthuma D. MAGMA: generalized gene-set  
734   analysis of GWAS data. *PLoS Comput Biol.* 2015;11:e1004219.

9. Sey NYA, Hu B, Mah W, Fauni H, McAfee JC, Rajarajan P, Brennand KJ, Akbarian S and Won H. A computational tool (H-MAGMA) for improved prediction of brain-disorder risk genes by incorporating brain chromatin interaction profiles. *Nat Neurosci.* 2020;23:583-593.
10. Jung I, Schmitt A, Diao Y, Lee AJ, Liu T, Yang D, Tan C, Eom J, Chan M, Chee S, Chiang Z, Kim C, Masliah E, Barr CL, Li B, Kuan S, Kim D and Ren B. A compendium of promoter-centered long-range chromatin interactions in the human genome. *Nat Genet.* 2019;51:1442-1449.
11. Pirruccello JP, Bick A, Wang M, Chaffin M, Friedman S, Yao J, Guo X, Venkatesh BA, Taylor KD, Post WS, Rich S, Lima JAC, Rotter JI, Philippakis A, Lubitz SA, Ellinor PT, Khera AV, Kathiresan S and Aragam KG. Analysis of cardiac magnetic resonance imaging in 36,000 individuals yields genetic insights into dilated cardiomyopathy. *Nat Commun.* 2020;11:2254.
12. Perrot A, Tomasov P, Villard E, Faludi R, Melacini P, Lossie J, Lohmann N, Richard P, De Bortoli M, Angelini A, Varga-Szemes A, Sperling SR, Simor T, Veselka J, Ozcelik C and Charron P. Mutations in NEBL encoding the cardiac Z-disk protein nebullette are associated with various cardiomyopathies. *Arch Med Sci.* 2016;12:263-78.
13. Jiang YH, Jiang LY, Wang YC, Ma DF and Li X. Quercetin Attenuates Atherosclerosis via Modulating Oxidized LDL-Induced Endothelial Cellular Senescence. *Front Pharmacol.* 2020;11:512.
14. Nock NL, Wang X, Thompson CL, Song Y, Baechle D, Raska P, Stein CM and Gray-McGuire C. Defining genetic determinants of the Metabolic Syndrome in the Framingham Heart Study using association and structural equation modeling methods. *BMC Proc.* 2009;3 Suppl 7:S50.

15. Motta M, Fasano G, Gredy S, Brinkmann J, Bonnard AA, Simsek-Kiper PO, Gulec EY, Essaddam L, Utine GE, Guarnetti Prandi I, Venditti M, Pantaleoni F, Radio FC, Ciolfi A, Petrini S, Consoli F, Vignal C, Hepbasli D, Ullrich M, de Boer E, Vissers L, Gritli S, Rossi C, De Luca A, Ben Becher S, Gelb BD, Dallapiccola B, Lauri A, Chillemi G, Schuh K, Cave H, Zenker M and Tartaglia M. SPRED2 loss-of-function causes a recessive Noonan syndrome-like phenotype. *Am J Hum Genet.* 2021;108:2112-2129.
16. Walters RG, Millwood IY, Lin K, Schmidt Valle D, McDonnell P, Hacker A, Avery D, Edris A, Fry H, Cai N, Kretzschmar WW, Ansari MA, Lyons PA, Collins R, Donnelly P, Hill M, Peto R, Shen H, Jin X, Nie C, Xu X, Guo Y, Yu C, Lv J, Clarke RJ, Li L, Chen Z and China Kadoorie Biobank Collaborative G. Genotyping and population characteristics of the China Kadoorie Biobank. *Cell Genom.* 2023;3:100361.
17. Zhou W, Kanai M, Wu KH, Rasheed H, Tsuo K, Hirbo JB, Wang Y, Bhattacharya A, Zhao H, Namba S, Surakka I, Wolford BN, Lo Faro V, Lopera-Maya EA, Lall K, Fave MJ, Partanen JJ, Chapman SB, Karjalainen J, Kurki M, Maasha M, Brumpton BM, Chavan S, Chen TT, Daya M, Ding Y, Feng YA, Guare LA, Gignoux CR, Graham SE, Hornsby WE, Ingold N, Ismail SI, Johnson R, Laisk T, Lin K, Lv J, Millwood IY, Moreno-Grau S, Nam K, Palta P, Pandit A, Preuss MH, Saad C, Setia-Verma S, Thorsteinsdottir U, Uzunovic J, Verma A, Zawistowski M, Zhong X, Afifi N, Al-Dabhani KM, Al Thani A, Bradford Y, Campbell A, Crooks K, de Bock GH, Damrauer SM, Douville NJ, Finer S, Fritsche LG, Fthenou E, Gonzalez-Arroyo G, Griffiths CJ, Guo Y, Hunt KA, Ioannidis A, Jansonius NM, Konuma T, Lee MTM, Lopez-Pineda A, Matsuda Y, Marioni RE, Moatamed B, Nava-Aguilar MA, Numakura K, Patil S, Rafaels N, Richmond A, Rojas-Munoz A, Shortt JA, Straub P, Tao R, Vanderwerff B, Vernekar M, Veturi Y, Barnes KC, Boezen M, Chen Z, Chen CY, Cho J, Smith GD, Finucane

780 HK, Franke L, Gamazon ER, Ganna A, Gaunt TR, Ge T, Huang H, Huffman J, Katsanis N,  
781 Koskela JT, Lajonchere C, Law MH, Li L, Lindgren CM, Loos RJF, MacGregor S, Matsuda K,  
782 Olsen CM, Porteous DJ, Shavit JA, Snieder H, Takano T, Trembath RC, Vonk JM, Whiteman  
783 DC, Wicks SJ, Wijmenga C, Wright J, Zheng J, Zhou X, Awadalla P, Boehnke M, Bustamante  
784 CD, Cox NJ, Fatumo S, Geschwind DH, Hayward C, Hveem K, Kenny EE, Lee S, Lin YF,  
785 Mbarek H, Magi R, Martin HC, Medland SE, Okada Y, Palotie AV, Pasaniuc B, Rader DJ,  
786 Ritchie MD, Sanna S, Smoller JW, Stefansson K, van Heel DA, Walters RG, Zollner S, Biobank  
787 of the A, Biobank Japan P, BioMe, BioVu, CanPath - Ontario Health S, China Kadoorie Biobank  
788 Collaborative G, Colorado Center for Personalized M, de CG, Estonian B, FinnGen, Generation  
789 S, Genes, Health Research T, LifeLines, Mass General Brigham B, Michigan Genomics I,  
790 National Biobank of K, Penn Medicine B, Qatar B, Sun QS, Health S, Taiwan B, Study H,  
791 Initiative UACH, Uganda Genome R, Biobank UK, Martin AR, Willer CJ, Daly MJ and Neale  
792 BM. Global Biobank Meta-analysis Initiative: Powering genetic discovery across human disease.  
793 *Cell Genom.* 2022;2:100192.

794 18. Aragam KG, Chaffin M, Levinson RT, McDermott G, Choi SH, Shoemaker MB, Haas  
795 ME, Weng LC, Lindsay ME, Smith JG, Newton-Cheh C, Roden DM, London B, Investigators  
796 G, Wells QS, Ellinor PT, Kathiresan S, Lubitz SA and Genetic Risk Assessment of Defibrillator  
797 Events I. Phenotypic Refinement of Heart Failure in a National Biobank Facilitates Genetic  
798 Discovery. *Circulation.* 2019;139:489-501.

799 19. Asai R, Kurihara Y, Fujisawa K, Sato T, Kawamura Y, Kokubo H, Tonami K, Nishiyama  
800 K, Uchijima Y, Miyagawa-Tomita S and Kurihara H. Endothelin receptor type A expression  
801 defines a distinct cardiac subdomain within the heart field and is later implicated in chamber  
802 myocardium formation. *Development.* 2010;137:3823-33.

- 803 20. Turley P, Walters RK, Maghzian O, Okbay A, Lee JJ, Fontana MA, Nguyen-Viet TA,  
804 Wedow R, Zacher M, Furlotte NA, andMe Research T, Social Science Genetic Association C,  
805 Magnusson P, Oskarsson S, Johannesson M, Visscher PM, Laibson D, Cesarini D, Neale BM  
806 and Benjamin DJ. Multi-trait analysis of genome-wide association summary statistics using  
807 MTAG. *Nat Genet.* 2018;50:229-237.
- 808 21. Ahlberg G, Andreassen L, Ghouse J, Bertelsen L, Bundgaard H, Haunso S, Svendsen JH  
809 and Olesen MS. Genome-wide association study identifies 18 novel loci associated with left  
810 atrial volume and function. *Eur Heart J.* 2021;42:4523-4534.
- 811 22. Pirruccello JP, Di Achille P, Nauffal V, Nekoui M, Friedman SF, Klarqvist MDR,  
812 Chaffin MD, Weng LC, Cunningham JW, Khurshid S, Roselli C, Lin H, Koyama S, Ito K,  
813 Kamatani Y, Komuro I, BioBank Japan P, Jurgens SJ, Benjamin EJ, Batra P, Natarajan P, Ng K,  
814 Hoffmann U, Lubitz SA, Ho JE, Lindsay ME, Philippakis AA and Ellinor PT. Genetic analysis  
815 of right heart structure and function in 40,000 people. *Nat Genet.* 2022;54:792-803.
- 816 23. Khurshid S, Lazarte J, Pirruccello JP, Weng LC, Choi SH, Hall AW, Wang X, Friedman  
817 SF, Nauffal V, Biddinger KJ, Aragam KG, Batra P, Ho JE, Philippakis AA, Ellinor PT and  
818 Lubitz SA. Clinical and genetic associations of deep learning-derived cardiac magnetic  
819 resonance-based left ventricular mass. *Nat Commun.* 2023;14:1558.
- 820 24. Nauffal V, Di Achille P, Klarqvist MDR, Cunningham JW, Hill MC, Pirruccello JP,  
821 Weng LC, Morrill VN, Choi SH, Khurshid S, Friedman SF, Nekoui M, Roselli C, Ng K,  
822 Philippakis AA, Batra P, Ellinor PT and Lubitz SA. Genetics of myocardial interstitial fibrosis in  
823 the human heart and association with disease. *Nat Genet.* 2023;55:777-786.

- 824 25. Kumar A, Ravi R, Sivakumar RK, Chidambaram V, Majella MG, Sinha S, Adamo L,  
825 Lau ES, Al'Aref SJ, Asnani A, Sharma G and Mehta JL. Prolactin Inhibition in Peripartum  
826 Cardiomyopathy: Systematic Review and Meta-analysis. *Curr Probl Cardiol.* 2023;48:101461.
- 827 26. Qu X, Harmelink C and Baldwin HS. Tie2 regulates endocardial sprouting and  
828 myocardial trabeculation. *JCI Insight.* 2019;5.
- 829 27. MacGrogan D, Munch J and de la Pompa JL. Notch and interacting signalling pathways  
830 in cardiac development, disease, and regeneration. *Nat Rev Cardiol.* 2018;15:685-704.
- 831 28. Knox C, Wilson M, Klinger CM, Franklin M, Oler E, Wilson A, Pon A, Cox J, Chin  
832 NEL, Strawbridge SA, Garcia-Patino M, Kruger R, Sivakumaran A, Sanford S, Doshi R,  
833 Khetarpal N, Fatokun O, Doucet D, Zubkowski A, Rayat DY, Jackson H, Harford K, Anjum A,  
834 Zakir M, Wang F, Tian S, Lee B, Liigand J, Peters H, Wang RQR, Nguyen T, So D, Sharp M, da  
835 Silva R, Gabriel C, Scantlebury J, Jasinski M, Ackerman D, Jewison T, Sajed T, Gautam V and  
836 Wishart DS. DrugBank 6.0: the DrugBank Knowledgebase for 2024. *Nucleic Acids Res.*  
837 2024;52:D1265-D1275.
- 838 29. Chen X, Ji ZL and Chen YZ. TTD: Therapeutic Target Database. *Nucleic Acids Res.*  
839 2002;30:412-5.
- 840 30. Zhou Y, Zhang Y, Lian X, Li F, Wang C, Zhu F, Qiu Y and Chen Y. Therapeutic target  
841 database update 2022: facilitating drug discovery with enriched comparative data of targeted  
842 agents. *Nucleic Acids Res.* 2022;50:D1398-D1407.
- 843 31. Chaugai S, Sherpa LY, Sepehry AA, Kerman SRJ and Arima H. Effects of Long- and  
844 Intermediate-Acting Dihydropyridine Calcium Channel Blockers in Hypertension: A Systematic  
845 Review and Meta-Analysis of 18 Prospective, Randomized, Actively Controlled Trials. *J*  
846 *Cardiovasc Pharmacol Ther.* 2018;23:433-445.



- 847 32. Packer M, McMurray JJV, Krum H, Kiowski W, Massie BM, Caspi A, Pratt CM, Petrie  
848 MC, DeMets D, Kobrin I, Roux S, Swedberg K, Investigators E and Committees. Long-Term  
849 Effect of Endothelin Receptor Antagonism With Bosentan on the Morbidity and Mortality of  
850 Patients With Severe Chronic Heart Failure: Primary Results of the ENABLE Trials. *JACC*  
851 *Heart Fail.* 2017;5:317-326.
- 852 33. Fradley MG, Nguyen NHK, Madnick D, Chen Y, DeMichele A, Makhlin I, Dent S,  
853 Lefebvre B, Carver J, Upshaw JN, DeRemer D, Ky B, Guha A and Gong Y. Adverse  
854 Cardiovascular Events Associated With Cyclin-Dependent Kinase 4/6 Inhibitors in Patients With  
855 Metastatic Breast Cancer. *J Am Heart Assoc.* 2023;12:e029361.
- 856 34. Frias JP, Davies MJ, Rosenstock J, Perez Manghi FC, Fernandez Lando L, Bergman BK,  
857 Liu B, Cui X, Brown K and Investigators S-. Tirzepatide versus Semaglutide Once Weekly in  
858 Patients with Type 2 Diabetes. *N Engl J Med.* 2021;385:503-515.
- 859 35. Rosenstock J, Wysham C, Frias JP, Kaneko S, Lee CJ, Fernandez Lando L, Mao H, Cui  
860 X, Karanikas CA and Thieu VT. Efficacy and safety of a novel dual GIP and GLP-1 receptor  
861 agonist tirzepatide in patients with type 2 diabetes (SURPASS-1): a double-blind, randomised,  
862 phase 3 trial. *Lancet.* 2021;398:143-155.
- 863 36. Sattar N, McGuire DK, Pavo I, Weerakkody GJ, Nishiyama H, Wiese RJ and Zoungas S.  
864 Tirzepatide cardiovascular event risk assessment: a pre-specified meta-analysis. *Nat Med.*  
865 2022;28:591-598.
- 866 37. Patel AP, Wang M, Ruan Y, Koyama S, Clarke SL, Yang X, Tcheandjie C, Agrawal S,  
867 Fahed AC, Ellinor PT, Genes, Health Research T, the Million Veteran P, Tsao PS, Sun YV, Cho  
868 K, Wilson PWF, Assimes TL, van Heel DA, Butterworth AS, Aragam KG, Natarajan P and

869 Khera AV. A multi-ancestry polygenic risk score improves risk prediction for coronary artery  
870 disease. *Nat Med.* 2023;29:1793-1803.

871 38. Wang Y, Namba S, Lopera E, Kerminen S, Tsuo K, Lall K, Kanai M, Zhou W, Wu KH,  
872 Fave MJ, Bhatta L, Awadalla P, Brumpton B, Deelen P, Hveem K, Lo Faro V, Magi R,  
873 Murakami Y, Sanna S, Smoller JW, Uzunovic J, Wolford BN, Global Biobank Meta-analysis I,  
874 Willer C, Gamazon ER, Cox NJ, Surakka I, Okada Y, Martin AR and Hirbo J. Global Biobank  
875 analyses provide lessons for developing polygenic risk scores across diverse cohorts. *Cell*  
876 *Genom.* 2023;3:100241.

877 39. Kanemaru K, Cranley J, Muraro D, Miranda AMA, Ho SY, Wilbrey-Clark A, Patrick  
878 Pett J, Polanski K, Richardson L, Litvinukova M, Kumasaka N, Qin Y, Jablonska Z, Semprich  
879 CI, Mach L, Dabrowska M, Richoz N, Bolt L, Mamanova L, Kapuge R, Barnett SN, Perera S,  
880 Talavera-Lopez C, Mulas I, Mahbubani KT, Tuck L, Wang L, Huang MM, Prete M, Pritchard S,  
881 Dark J, Saeb-Parsy K, Patel M, Clatworthy MR, Hubner N, Chowdhury RA, Nosedà M and  
882 Teichmann SA. Spatially resolved multiomics of human cardiac niches. *Nature.* 2023;619:801-  
883 810.

884 40. Baig SM, Koschak A, Lieb A, Gebhart M, Dafinger C, Nurnberg G, Ali A, Ahmad I,  
885 Sinnegger-Brauns MJ, Brandt N, Engel J, Mangoni ME, Farooq M, Khan HU, Nurnberg P,  
886 Striessnig J and Bolz HJ. Loss of Ca(v)1.3 (CACNA1D) function in a human channelopathy  
887 with bradycardia and congenital deafness. *Nat Neurosci.* 2011;14:77-84.

888 41. Herman DS, Lam L, Taylor MR, Wang L, Teekakirikul P, Christodoulou D, Conner L,  
889 DePalma SR, McDonough B, Sparks E, Teodorescu DL, Cirino AL, Banner NR, Pennell DJ,  
890 Graw S, Merlo M, Di Lenarda A, Sinagra G, Bos JM, Ackerman MJ, Mitchell RN, Murry CE,

891 Lakdawala NK, Ho CY, Barton PJ, Cook SA, Mestroni L, Seidman JG and Seidman CE.  
892 Truncations of titin causing dilated cardiomyopathy. *N Engl J Med*. 2012;366:619-28.

893 42. Nagai A, Hirata M, Kamatani Y, Muto K, Matsuda K, Kiyohara Y, Ninomiya T,  
894 Tamakoshi A, Yamagata Z, Mushiroda T, Murakami Y, Yuji K, Furukawa Y, Zembutsu H,  
895 Tanaka T, Ohnishi Y, Nakamura Y, BioBank Japan Cooperative Hospital G and Kubo M.  
896 Overview of the BioBank Japan Project: Study design and profile. *J Epidemiol*. 2017;27:S2-S8.

897 43. Delaneau O, Zagury JF, Robinson MR, Marchini JL and Dermitzakis ET. Accurate,  
898 scalable and integrative haplotype estimation. *Nat Commun*. 2019;10:5436.

899 44. Das S, Forer L, Schonherr S, Sidore C, Locke AE, Kwong A, Vrieze SI, Chew EY, Levy  
900 S, McGue M, Schlessinger D, Stambolian D, Loh PR, Iacono WG, Swaroop A, Scott LJ, Cucca  
901 F, Kronenberg F, Boehnke M, Abecasis GR and Fuchsberger C. Next-generation genotype  
902 imputation service and methods. *Nat Genet*. 2016;48:1284-1287.

903 45. Mbatchou J, Barnard L, Backman J, Marcketta A, Kosmicki JA, Ziyatdinov A, Benner C,  
904 O'Dushlaine C, Barber M, Boutkov B, Habegger L, Ferreira M, Baras A, Reid J, Abecasis G,  
905 Maxwell E and Marchini J. Computationally efficient whole-genome regression for quantitative  
906 and binary traits. *Nat Genet*. 2021;53:1097-1103.

907 46. Zhang L, Ono Y, Qiao Q and Nagai T. Trends in heart failure prevalence in Japan 2014-  
908 2019: a report from healthcare administration databases. *ESC Heart Fail*. 2023;10:1996-2009.

909 47. Ide T, Kaku H, Matsushima S, Tohyama T, Enzan N, Funakoshi K, Sumita Y, Nakai M,  
910 Nishimura K, Miyamoto Y, Tsuchihashi-Makaya M, Hatano M, Komuro I, Tsutsui H and  
911 Investigators J. Clinical Characteristics and Outcomes of Hospitalized Patients With Heart  
912 Failure From the Large-Scale Japanese Registry Of Acute Decompensated Heart Failure  
913 (JROADHF). *Circ J*. 2021;85:1438-1450.

48. Gusev A, Ko A, Shi H, Bhatia G, Chung W, Penninx BW, Jansen R, de Geus EJ, Boomsma DI, Wright FA, Sullivan PF, Nikkola E, Alvarez M, Civelek M, Lusi AJ, Lehtimäki T, Raitoharju E, Kahonen M, Seppälä I, Raitakari OT, Kuusisto J, Laakso M, Price AL, Pajukanta P and Pasaniuc B. Integrative approaches for large-scale transcriptome-wide association studies. *Nat Genet.* 2016;48:245-52.
49. Aragam KG, Jiang T, Goel A, Kanoni S, Woldford BN, Atri DS, Weeks EM, Wang M, Hindy G, Zhou W, Grace C, Roselli C, Marston NA, Kamanu FK, Surakka I, Venegas LM, Sherliker P, Koyama S, Ishigaki K, Asvold BO, Brown MR, Brumpton B, de Vries PS, Giannakopoulou O, Giardoglou P, Gudbjartsson DF, Guldener U, Haider SMI, Helgadóttir A, Ibrahim M, Kastrati A, Kessler T, Kyriakou T, Konopka T, Li L, Ma L, Meitinger T, Mucha S, Munz M, Murgia F, Nielsen JB, Nothen MM, Pang S, Reinberger T, Schnitzler G, Smedley D, Thorleifsson G, von Scheidt M, Ulirsch JC, Biobank J, Epic CVD, Arnar DO, Burt NP, Costanzo MC, Flannick J, Ito K, Jang DK, Kamatani Y, Khera AV, Komuro I, Kullo IJ, Lotta LA, Nelson CP, Roberts R, Thorgeirsson G, Thorsteinsdóttir U, Webb TR, Baras A, Björkegren JLM, Boerwinkle E, Dedoussis G, Holm H, Hveem K, Melander O, Morrison AC, Orho-Melander M, Rallidis LS, Ruusalepp A, Sabatine MS, Stefansson K, Zalloua P, Ellinor PT, Farrall M, Danesh J, Ruff CT, Finucane HK, Hopewell JC, Clarke R, Gupta RM, Erdmann J, Samani NJ, Schunkert H, Watkins H, Willer CJ, Deloukas P, Kathiresan S, Butterworth AS and Consortium CAD. Discovery and systematic characterization of risk variants and genes for coronary artery disease in over a million participants. *Nat Genet.* 2022;54:1803-1815.

## Figures

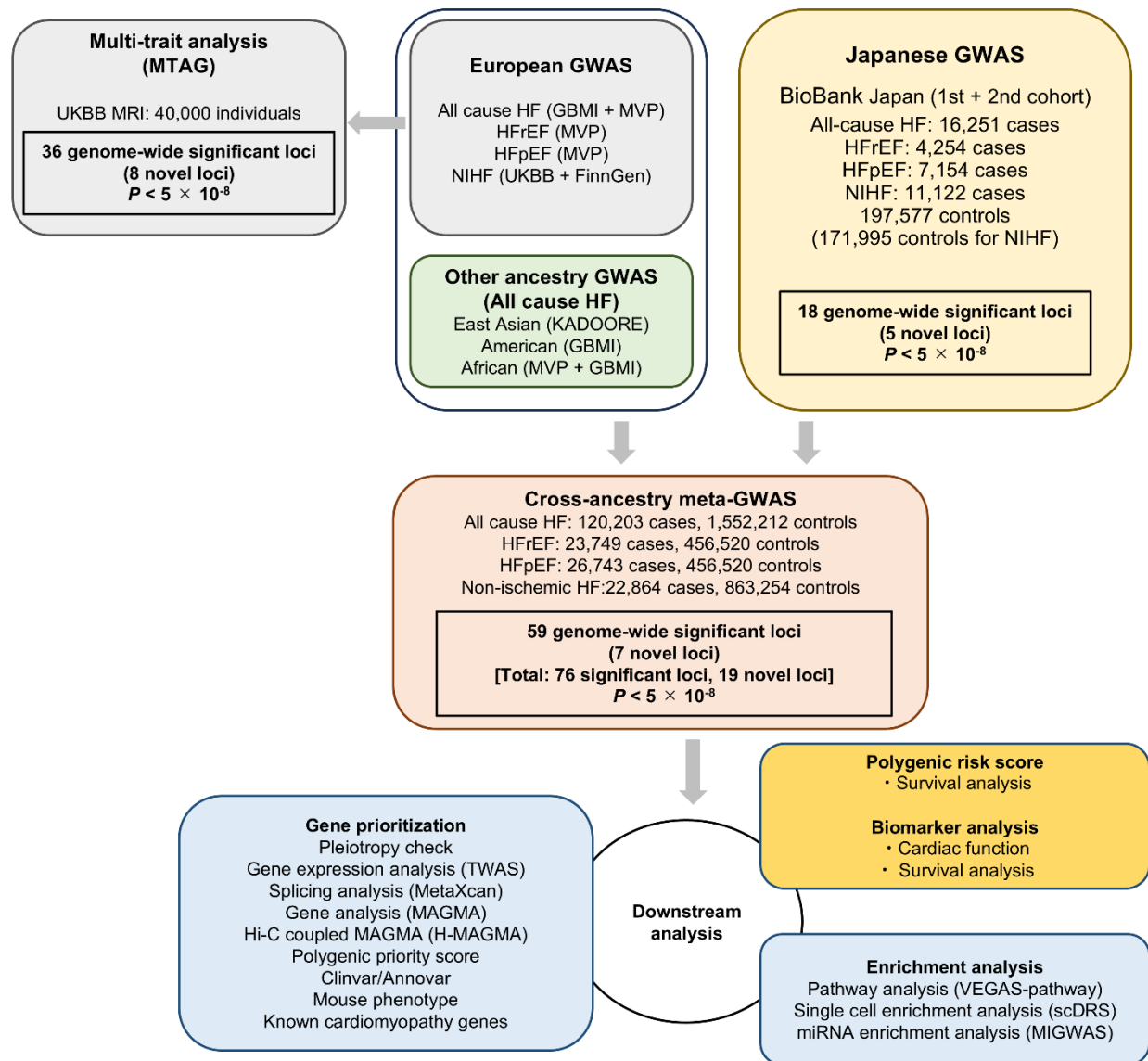


**Fig. 1 | Overview of the study design.** Flowchart of the study, which encompasses the Japanese GWAS with the BioBank Japan, a trans-ancestry meta-analysis with large-scale European and other population GWAS followed by the downstream analysis. GWAS, genome wide association study; HF, heart failure; HFpEF, heart failure with preserved ejection fraction; HFrEF, heart failure with reduced ejection fraction; NIHF; non-ischemic heart failure; TWAS, transcriptome-wide association study.

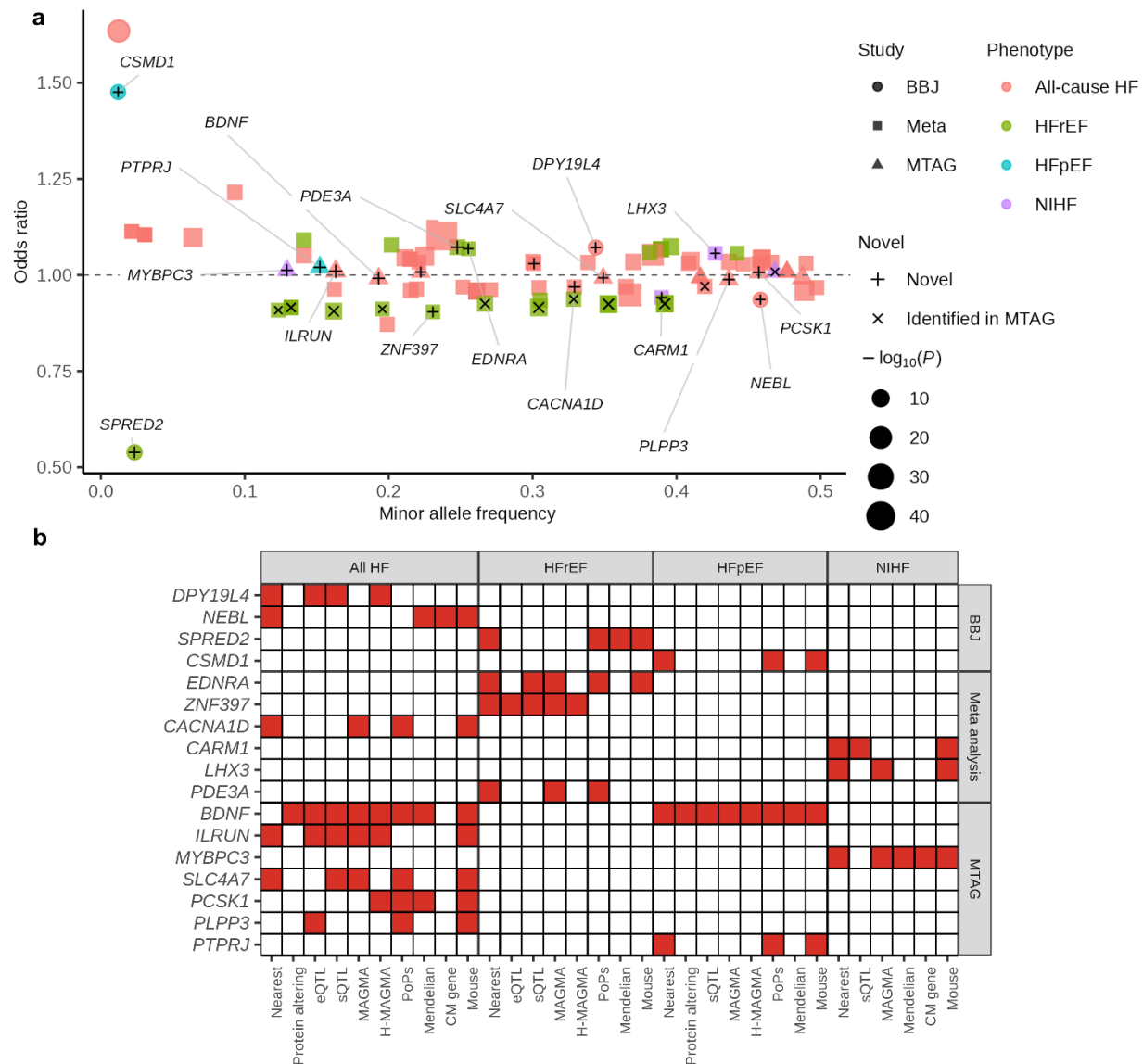


**Fig. 2 | Prioritized genes.** (a) The odds ratios for HF development of the independent signals in the Japanese GWAS, cross-ancestry meta-analysis, and MTAG. The color of each point indicates the corresponding HF phenotype. The size of each point indicates  $-\log_{10}(P)$  value. The shape of each point indicates the methods of analysis. The marker inside each point indicates novelty status. (b) Prioritized genes for each HF phenotype according to the types of analyses. *CACNA1D* was prioritized in both BBJ and cross-ancestry meta-analysis and is shown in the “Meta-analysis” row. BBJ, BioBank Japan; HF, heart failure; HFpEF, heart failure with

952    preserved ejection fraction; HFrEF, heart failure with reduced ejection fraction; Meta, meta-  
953    analysis; MTAG, multi-trait analysis of genome-wide association study; NIHF, non-ischemic  
954    heart failure.

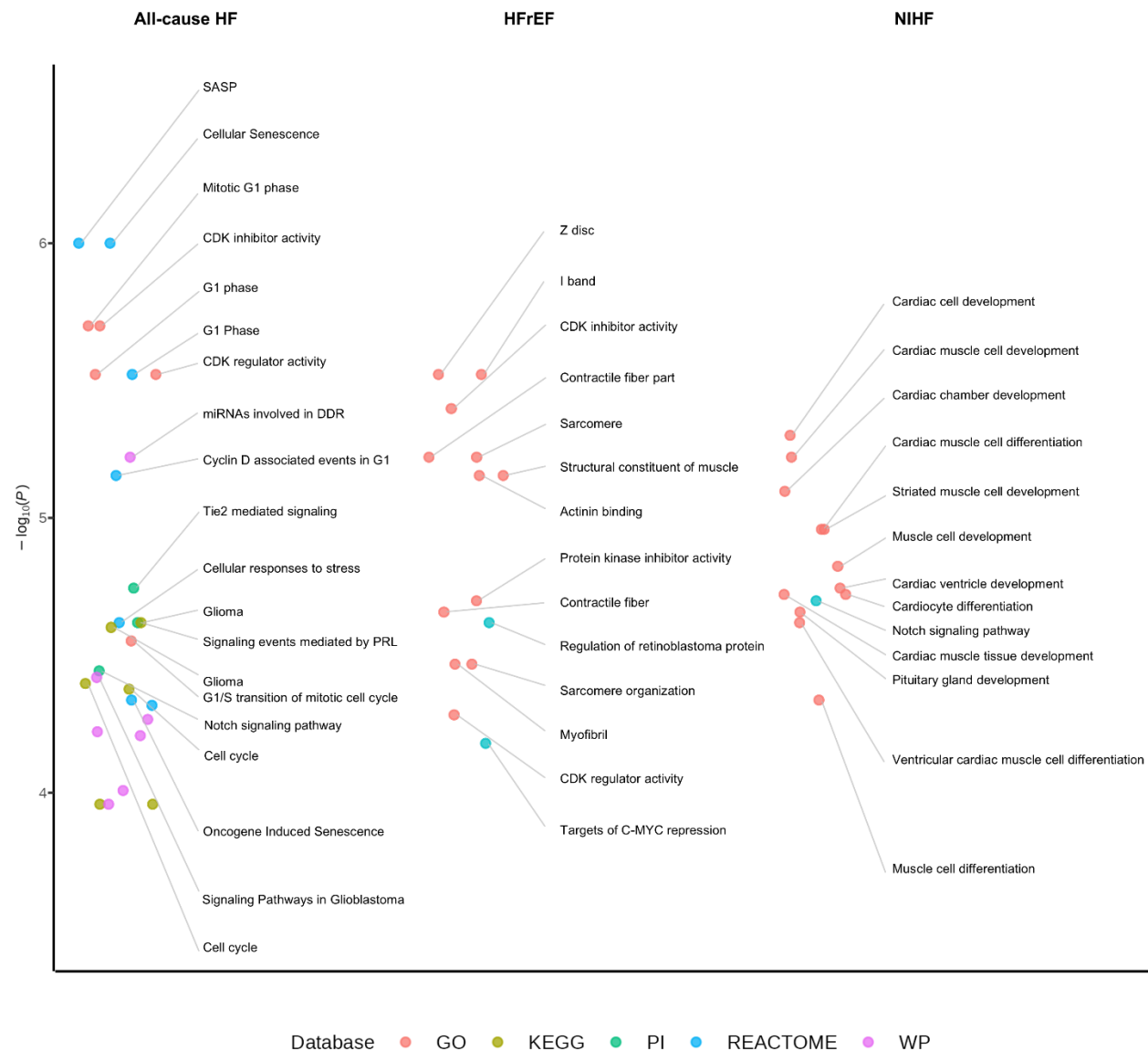


**Fig. 3 | Pathway analysis for each HF phenotype.** Enriched terms (FDR < 0.05) for each HF phenotype from GO, KEGG, PI, Reactome, and WP. Up to the top 20 enriched terms in each HF phenotype gene set are labeled. The color of the dots indicates the pathway. There was no enriched pathway for HFpEF. GO, Gene Ontology; KEGG, Kyoto Encyclopedia of Genes and Genomes; PI, Pathway Interaction database; WP, Wiki Pathways.



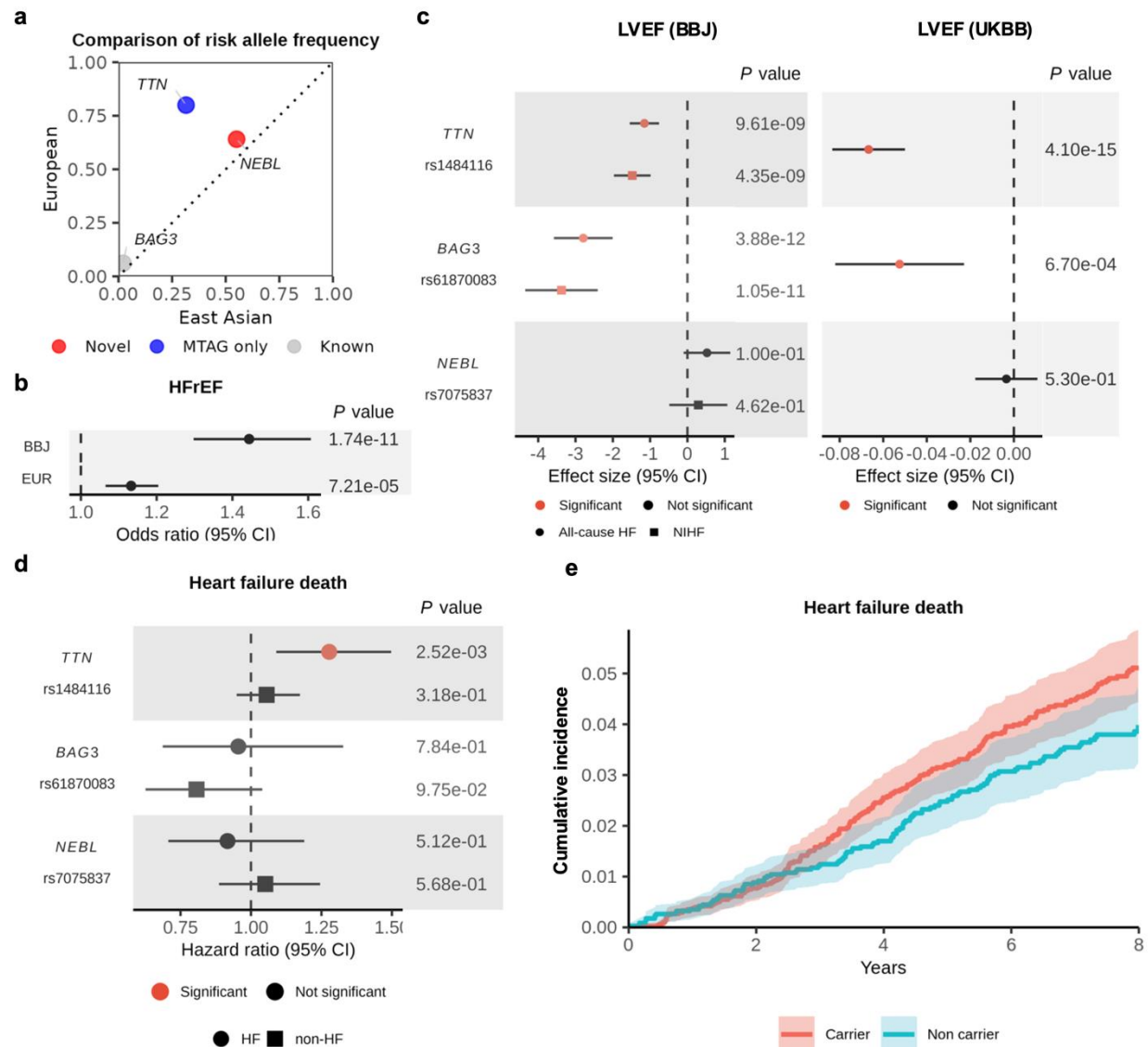


**Fig. 4 | Effects of common variants in cardiomyopathy genes on left ventricular function and long-term HF mortality. (a)** Minor allele frequency of lead SNPs in cardiomyopathy genes for East Asian and European populations according to gnomAD. **(b)** Effect size comparison of rs148116 (*TTN*) between BBJ and European for HFrEF. **(c)** Effects of lead variants in cardiomyopathy genes on LVEF in BBJ cohorts (left panel) and UKBB cohorts (right panel). Data are presented as estimated coefficients and their 95% confidence interval (CI). The shape of the points in c and d indicates the HF subtypes. Red points in c and d indicate statistically

969 significant effects. HF, heart failure; NIHF, non-ischemic heart failure. **(d)** Effects of lead  
970 variants in cardiomyopathy genes for HF mortality among HF patients (indicated as circles, ICD-  
971 10 I50, 326 deaths among 8,481 individuals) and non-HF individuals (indicated as squares, ICD-  
972 10 I50, 749 deaths among 121,070 individuals). **(e)** Cumulative incidence curve for HF death  
973 according to carriers of rs1484116 (*TTN*) in HF patients.

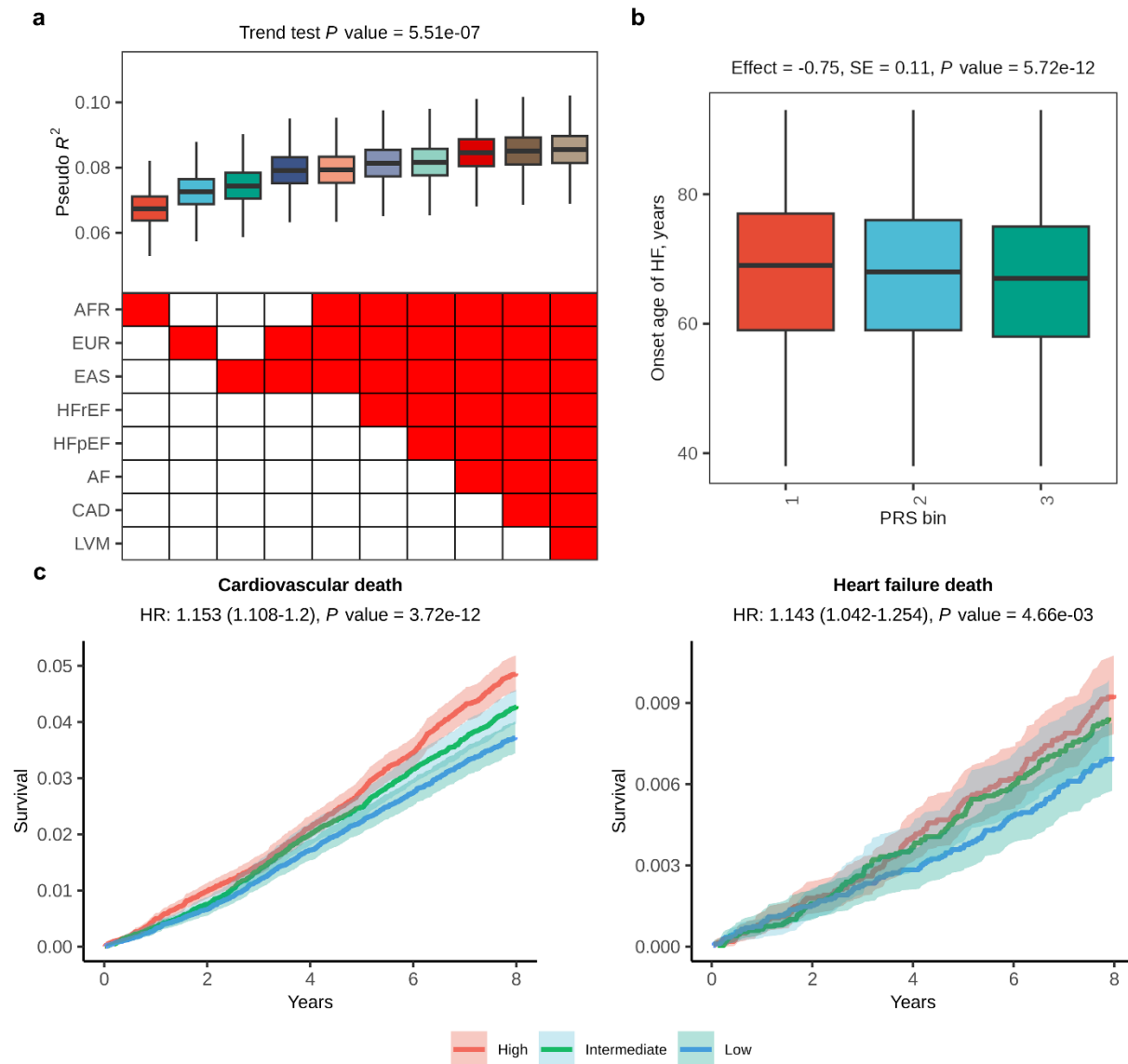


**Fig. 5 | Performance and clinical impact of the HF-PRS.** (a) Each point indicates Nagelkerke's pseudo  $R^2$  for all-cause HF case-control status in the Japanese independent cohort (1,837 cases and 11,319 controls). PRS-derivation cohorts are indicated on the x-axis. (b) Association between HF-PRS and onset age of HF. The onset age of HF in individuals with data available ( $n = 10,810$ ) is shown based on the HF-PRS tertiles. The number of individuals in each tertile is 3,603 to 3,604. The center line of the box plot indicates the median, the bounds represent the first and third quartile, and the whiskers reach to 1.5 times the interquartile range.

982 (c) Kaplan-Meier estimates of cumulative events from cardiovascular mortality (left) and HF  
983 death (right) are shown with a band of 95%CI. Individuals are classified into high (top tertile),  
984 intermediate (middle tertile), and low PRS (bottom tertile). P values were calculated for PRS by  
985 Cox proportional hazard analysis and the significance was set at  $P = 8.3 \times 10^{-3}$  (0.05/6).

# Genome-wide analysis of heart failure enables polygenic and monogenic prediction of heart failure risks

## Table of Contents

<b>Supplementary Notes</b>	<b>3</b>
<b>1. The SNP heritability and the liability-scale heritability</b>	<b>3</b>
<b>2. Replication of previously identified HF risk loci</b>	<b>3</b>
<b>3. Internal and external replication for novel loci found in BBJ GWAS</b>	<b>3</b>
<b>4. Cohorts used for cross-ancestry meta-analyses</b>	<b>4</b>
<b>5. Internal and external replication of cross-ancestry meta-analyses results</b>	<b>5</b>
<b>6. Prioritization of rs10851802 in the cross-ancestry meta-analyses</b>	<b>5</b>
<b>7. Prioritized genes in MTAG</b>	<b>5</b>
<b>Supplementary methods</b>	<b>6</b>
<b>Cohort characteristics for BBJ 1<sup>st</sup> cohort and BBJ 2<sup>nd</sup> cohort</b>	<b>6</b>
<b>Cell type-specific heritability enrichment of disease associations</b>	
<b>using stratified LD score regression</b>	<b>7</b>
<b>Links between medication and prioritized loci</b>	<b>7</b>
<b>miRNA enrichment analysis</b>	<b>8</b>
<b>Heritability enrichment with scDRS</b>	<b>8</b>
<b>Supplementary Figures</b>	<b>9</b>
<b>Supplementary Fig. 1   Results of Japanese GWAS</b>	<b>9</b>
<b>Supplementary Fig. 2   Validation of previously identified loci using BBJ</b>	<b>10</b>
<b>Supplementary Fig. 3   Comparison of allele frequencies and</b>	

26	<b>allelic effects identified in Japanese GWAS .....</b>	<b>11</b>
27	<b>Supplementary Fig. 4   Downstream analysis of Japanese GWAS .....</b>	<b>13</b>
28	<b>Supplementary Fig. 5   Phenogram of genome-wide significant loci for HF</b>	
29	<b>and its subtypes .....</b>	<b>15</b>
30	<b>Supplementary Fig. 6   Results of the cross-ancestry meta-analysis .....</b>	<b>16</b>
31	<b>Supplementary Fig. 7   QQ plot and comparison of allele frequencies</b>	
32	<b>and allelic effects identified in the cross-ancestry meta-analysis .....</b>	<b>17</b>
33	<b>Supplementary Fig. 8   Downstream analysis of</b>	
34	<b>cross-ancestry meta-analysis .....</b>	<b>19</b>
35	<b>Supplementary Fig. 9   Results of multi-trait analysis of GWAS .....</b>	<b>21</b>
36	<b>Supplementary Fig. 10   Downstream analysis of</b>	
37	<b>multi-trait analysis of GWAS .....</b>	<b>23</b>
38	<b>Supplementary Fig. 11   Benn diagram for genes identified by each analysis ..</b>	<b>25</b>
39	<b>Supplementary Fig. 12   miRNA enrichment analysis and</b>	
40	<b>Single-cell enrichment analysis .....</b>	<b>26</b>
41	<b>Supplementary Fig. 13   Candidate drugs linked to disease</b>	
42	<b>susceptibility loci for HF.....</b>	<b>27</b>
43	<b>Supplementary Fig. 14   Analytical scheme for PRS development .....</b>	<b>28</b>
44	<b>Supplementary Fig. 15   PRS performance .....</b>	<b>29</b>
45	<b>Members of participating consortia .....</b>	<b>30</b>
46	<b>References .....</b>	<b>33</b>

47

## Supplementary Notes

### 1. The SNP heritability and the liability-scale heritability

The proportion of the variation in HF phenotypes (the single nucleotide polymorphism (SNP) heritability;  $h^2$ ) was estimated to be 1.5% (standard error of the mean [s.e.m.] 0.3%) for all-cause HF, 1.5% (0.3%) for HFrEF, 0.5% (0.3%) for HFpEF, and 1.1% (0.3%) for NIHF using linkage disequilibrium (LD)-score regression (LDSC). The liability-scale  $h^2$  was estimated at 4.8% (s.e.m. 1.0%) for all-cause HF, 12.6% (2.9%) for HFrEF, 2.8% (1.7%) for HFpEF, and 3.1% (1.0%) for NIHF, suggesting the heterogeneous heritability in each HF phenotype.

### 2. Replication of previously identified HF risk loci

We assessed the 47 independent variants previously reported from all-cause HF GWAS<sup>1</sup>, 13 variants from HFrEF GWAS, one variant from HFpEF GWAS<sup>2</sup>, and one variant from NIHF<sup>3</sup> in our Japanese GWAS (BBJ). Out of 47 variants identified in the previous all-cause HF GWAS, 34 variants or variants tagged with the lead variant existed in BBJ, 28 had the same effect direction, and 18 were nominally significant ( $P < 0.05$ ; **Supplementary Fig. 2, Supplementary Table 3**). Out of 13 variants identified in the European HFrEF GWAS, 11 existed in BBJ, 10 had the same effect direction, and 3 were nominally significant. The lead variant identified in the European HFpEF GWAS had the same direction and was nominally significant in BBJ, and the lead or tagged variant identified in the European NIHF GWAS did not exist in BBJ.

### 3. Internal and external replication for novel loci found in BBJ GWAS

We sought to replicate the HF-risk loci that reached genome-wide significance in individual GWAS cohorts. The effect size, direction (**Supplementary Fig. 3a**), and allele frequency of the

identified lead variants (**Supplementary Figure 3b**) were strongly concordant in BBJ 1<sup>st</sup> and BBJ 2<sup>nd</sup> cohorts for all HF phenotypes (Pearson's correlation: all-cause HF 0.981; HFrEF 0.961; HFpEF 0.752; NIHF 0.992). Three out of the five newly identified loci were nominally significant in both BBJ 1<sup>st</sup> and BBJ 2<sup>nd</sup> cohorts (**Supplementary Fig. 3a** and **Supplementary Table 4**). Out of the five newly identified loci, three loci identified in all-cause HF were found in the European GWAS. rs35593046 were successfully replicated with nominal association ( $P < 0.05$ ) with the same effect direction (**Supplementary Fig. 3c** and **Supplementary Table 5**). As for rs6471480 and rs7075837, the same effect direction was observed in the European population. rs76704104 identified in HFrEF and rs78228190 identified in HFpEF were not observed in the European population according to the Genome Aggregation Database v4.0.0 (gnomAD) (<https://gnomad.broadinstitute.org/>).

#### 4. Cohorts used for cross-ancestry meta-analyses

Cross-ancestry datasets (**Supplementary Table 18**) yielded 120,203 cases for all-cause HF (BBJ: 16,251, EUR: 95,524, KADOORIE: 1,467, AMR: 1,170, AFR: 5,791), 23,749 cases for HFrEF (BBJ 4,254, EUR: 19,495), 26,743 cases for HFpEF (BBJ: 7,154, EUR: 19,589), and 22,864 cases for NIHF (BBJ: 11,122, UKBB: 1,816, FinnGen: 9,926). The number of control samples was 1,502,645 (BBJ: 197,577, EUR: 1,270,968, KADOORIE: 75,149, AMR: 13,217, AFR: 20,883) for all-cause HF, 456,520 for HFrEF/HFpEF (BBJ: 197,577, EUR: 258,943), and 863,254 for NIHF (BBJ: 171,995, UKBB: 387,652, FinnGen: 303,607), respectively. We included variants with  $MAF \geq 1\%$  and tested a total of 11,119,536 variants for all-cause HF, 4,800,324 variants for HFrEF, 4,807,066 variants for HFpEF, and 4,998,828 variants for NIHF.



## 5. Internal and external replication of cross-ancestry meta-analyses results

The effect size and direction of the identified lead variants (**Supplementary Fig. 7b**) were concordant in East Asians and Europeans for all HF phenotypes (Pearson's correlation: all-cause HF 0.898; HFrEF 0.864; NIHF 0.983) except for HFpEF, for which Pearson's correlation could not be calculated with significant loci < 3.

To replicate lead variants of HFrEF and HFpEF using independent datasets, these were assessed with European all-cause HF GWAS since there were no other available HFrEF/HFpEF GWAS datasets. As for all-cause HF and NIHF, there was no dataset for external replication. Effect sizes were generally concordant with Pearson's correlation of 0.817 in HFrEF (**Supplementary Figure 7d and e**). The effect direction was also concordant in all of the three novel loci (**Supplementary Table 21**). As for HFpEF, both significant variants were known HF-related variants.

## 6. Prioritization of rs10851802 in the cross-ancestry meta-analyses

Among novel loci, we could not prioritize a gene for rs10851802. rs10851802 is linked to *GLCE* according to the Open Targets database. rs10851802 was associated with rs2415040 ( $r^2 = 0.548$ ), which was a variant for lean mass<sup>4</sup>. Lean mass is associated with incident HF<sup>5</sup>. Although we could not prioritize a gene in this locus, this evidence suggests that this locus was one of the disease susceptibility loci. Further investigations were warranted to identify the candidate gene in this locus.

## 7. Prioritized genes in MTAG

*BDNF* prioritized by PoPS (**Supplementary Table 40**) harbored pathogenic variants responsible for obesity (**Supplementary Table 38**), and its knockout showed the same phenotype (**Supplementary Table 39**). *MYBPC3* was one of the known cardiomyopathy genes (**Supplementary Table 14, 38 and 39**), and this is the first report to show that common variants of *MYBPC3* were associated with HF. *SLC4A7*, prioritized by PoPS (**Supplementary Table 40**), was associated with abnormal vasoconstriction (**Supplementary Table 39**). Considering *SLC4A7* splicing was enriched in fibroblasts (**Supplementary Figure 10b**), it suggested that arterial fibroblasts contributed to HF through hypertension. Common variants in *PCSK1* influenced blood pressure<sup>6</sup>, which was consistent with the fact that *PCSK1* was prioritized H-MAGMA using the aorta Hi-C dataset (**Supplementary Fig. 10c**) and *PCSK1* knockout showed obesity and hypertension (**Supplementary Table 39**). *PTPRJ* knockout showed abnormal vascular development and abnormal heart development (**Supplementary Table 39**). *PLPP3* was enriched in the fibroblasts in TWAS (**Figure 10a**), and its knockout caused the abnormal vasculogenesis. These results were consistent with the previous report which indicated that *PLPP3* regions was associated with hypertension<sup>7</sup> and coronary artery disease<sup>8</sup>.

Among the novel loci, we could not assign a gene to rs10888955. This variant was strongly associated with reticulocyte count<sup>9</sup>. Given that previous Mendelian randomization analysis revealed the positive association of CAD with reticulocytes<sup>10</sup>, this locus could contribute to HF development through CAD.

## Supplementary methods

### Cohort characteristics for BBJ 1<sup>st</sup> cohort and BBJ 2<sup>nd</sup> cohort

All subjects were Japanese and were registered in the BioBank Japan (BBJ) project (<https://biobankjp.org/>). The BBJ is a hospital-based national biobank project that collects DNA and serum samples and clinical information from 12 cooperative medical institutes throughout Japan (Osaka Medical Center for Cancer and Cardiovascular Diseases, Cancer Institute Hospital of Japanese Foundation for Cancer Research, Juntendo University, Tokyo Metropolitan Geriatric Hospital, Nippon Medical School, Nihon University School of Medicine, Iwate Medical University, Tokushukai Hospitals, Shiga University of Medical Science, Fukujiji Hospital, National Hospital Organization Osaka National Hospital, and Iizuka Hospital). Approximately 267,000 patients with any of the 47 target diseases were enrolled from 2003 to 2007, and from 2013 to 2018. All subjects were at least 18 years old. Informed consent was obtained from all participants, and our study was approved by the relevant ethical committee at each facility.

## **Cell type-specific heritability enrichment of disease associations using stratified LD score regression**

We applied stratified LD score regression (S-LDSC)<sup>11</sup> (v1.0.1. <https://github.com/bulik/ldsc>) to the GWAS summary statistics of the cross-ancestry meta-analysis to evaluate the contribution of genetic variation in cell type-specific genes to trait heritability. Heritability enrichment per cell type was considered significant at  $P < 7.2 \times 10^{-5}$  (0.05/694) based on the number of cell types tested (694).

## **Links between medication and prioritized loci**

We searched medications linked to prioritized genes using DrugBank and the Therapeutic Target Database. Among medications with the same pharmacological actions, we chose a representative

one manually. The role of prioritized genes (e.g. protective or detrimental against HF) was determined based on (1) knockout mice phenotyping or (2) the direction of TWAS Z-score if knockout mice phenotyping was not reported to be associated with HF.

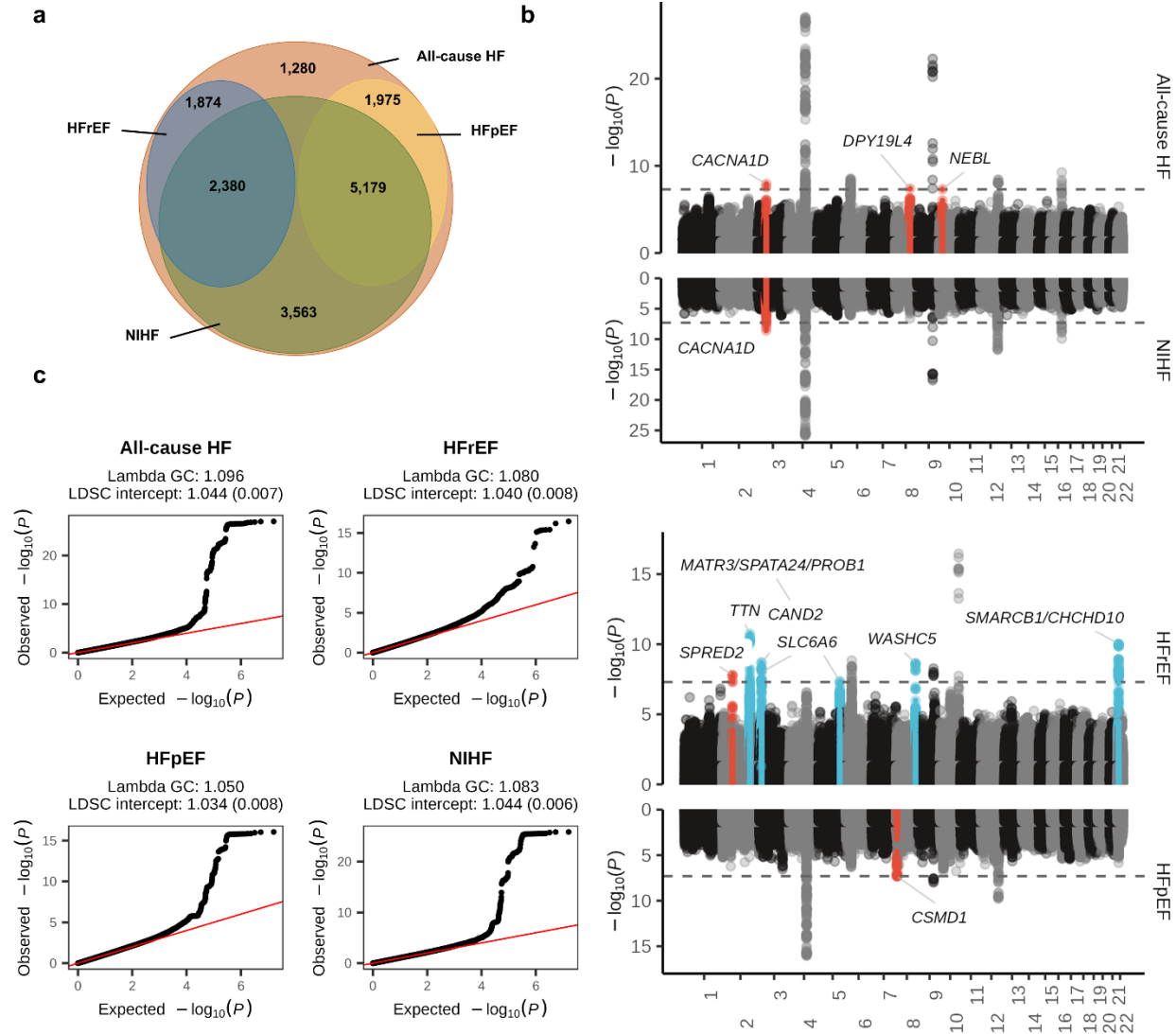
### **miRNA enrichment analysis**

The overall polygenic contribution of miRNA–target gene network to the traits through the tissue-naïve approach was estimated using MIGWAS software with default settings<sup>12</sup>. The significance threshold was set at 0.0125 based on the number of HF phenotypes (0.05/4). Candidate miRNA-gene pairs were estimated by MIGWAS with a significance threshold set at FDR < 0.05 for miRNA and genes.

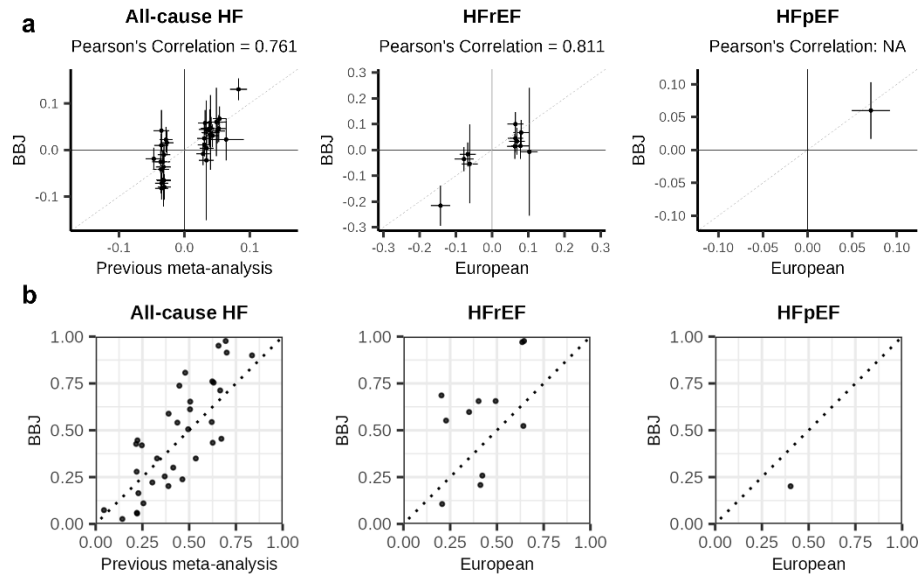
### **Heritability enrichment with scDRS**

To determine which cell types in hearts were enriched for HF GWAS, we used scDRS (v.1.0.2)<sup>13</sup> with default settings. We used MAGMA v.1.10<sup>14</sup> to map single-nucleotide polymorphisms to genes (GRCh37 genome build from the 1000 Genomes Project) using an annotation window of 0 kb. We used the resulting annotations and GWAS summary statistics to calculate each gene's MAGMA z score (association with a given trait). The 1,000 disease genes used for scDRS were chosen and weighted based on their top MAGMA z scores. To determine trait association at the annotated cell type resolution, we used the z scores computed from scDRS's downstream Monte Carlo test. These Monte Carlo z scores were converted to theoretical P values using a one-sided test under a normal distribution. The significance threshold was set at  $P < 2.4 \times 10^{-3}$  based on Bonferroni correction (0.05/21 based on the number of cell types).

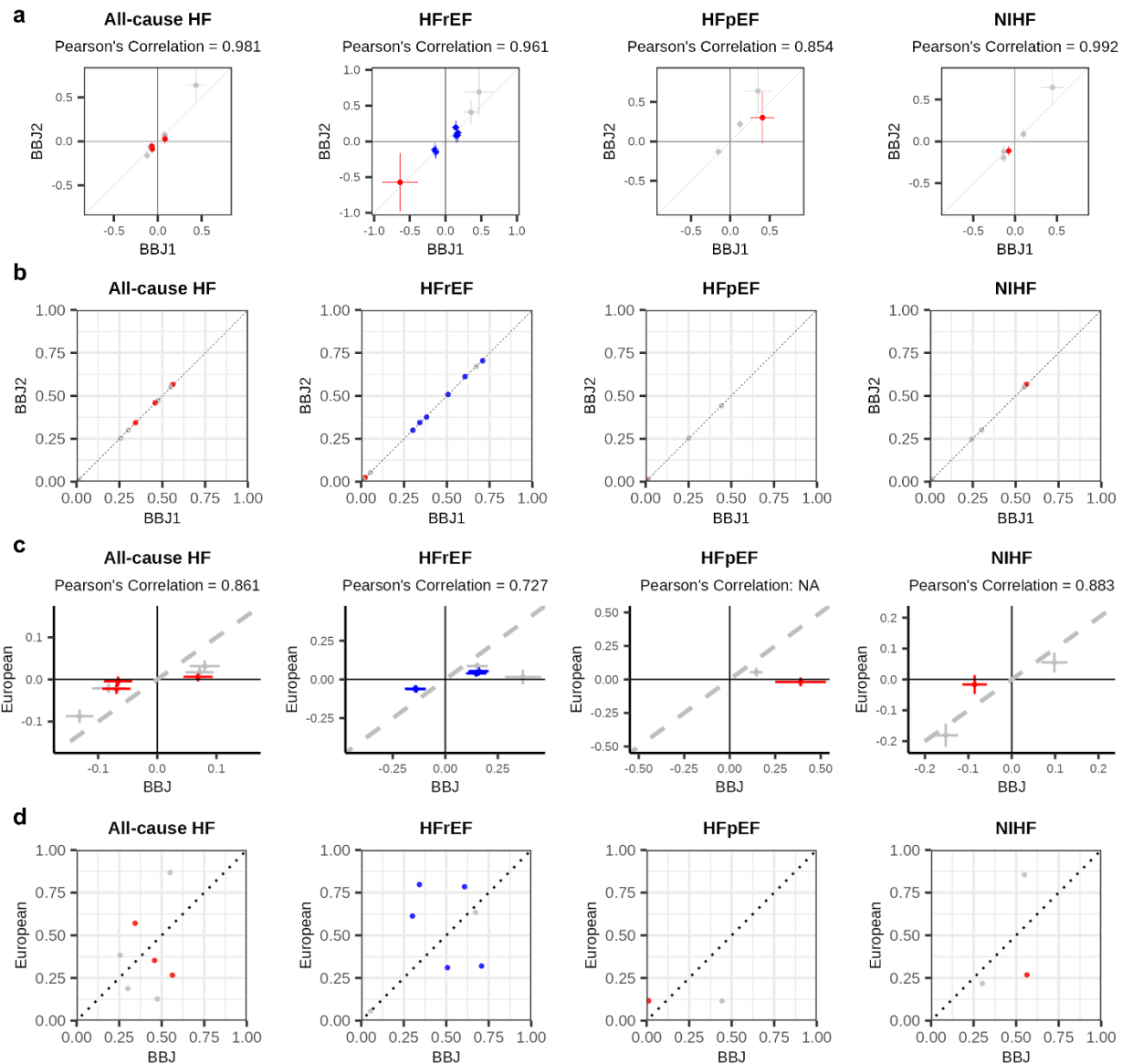
## Supplementary Figures



**Supplementary Fig. 1 | Results of Japanese GWAS.** (a) Sample overlap between each HF phenotype in Japanese GWAS. (b) Miami plot for four HF phenotypes.  $-\log_{10}(P)$  value on the y-axis are shown against the genomic positions (hg19) on the x-axis. Association signals that reached a genome-wide significance level ( $P < 5 \times 10^{-8}$ ) are shown in red if new loci and in blue if previously reported only in MTAG but not in GWAS. (c) QQ plot for each HF phenotype in Japanese GWAS. Two-sided  $P$  values were calculated using a logistic regression model. GWAS, genome-wide association study; HF, heart failure; MTAG, multi-trait analysis of GWAS.



**Supplementary Fig. 2 | Validation of previously identified HF loci in BBJ.** Comparison of allelic effects (a) and allele frequency (b) between the previous GWAS and BBJ. Effect size with its 95%CI or allele frequency of previous GWAS are shown in the x-axis, and those of BBJ are shown in the y-axis.



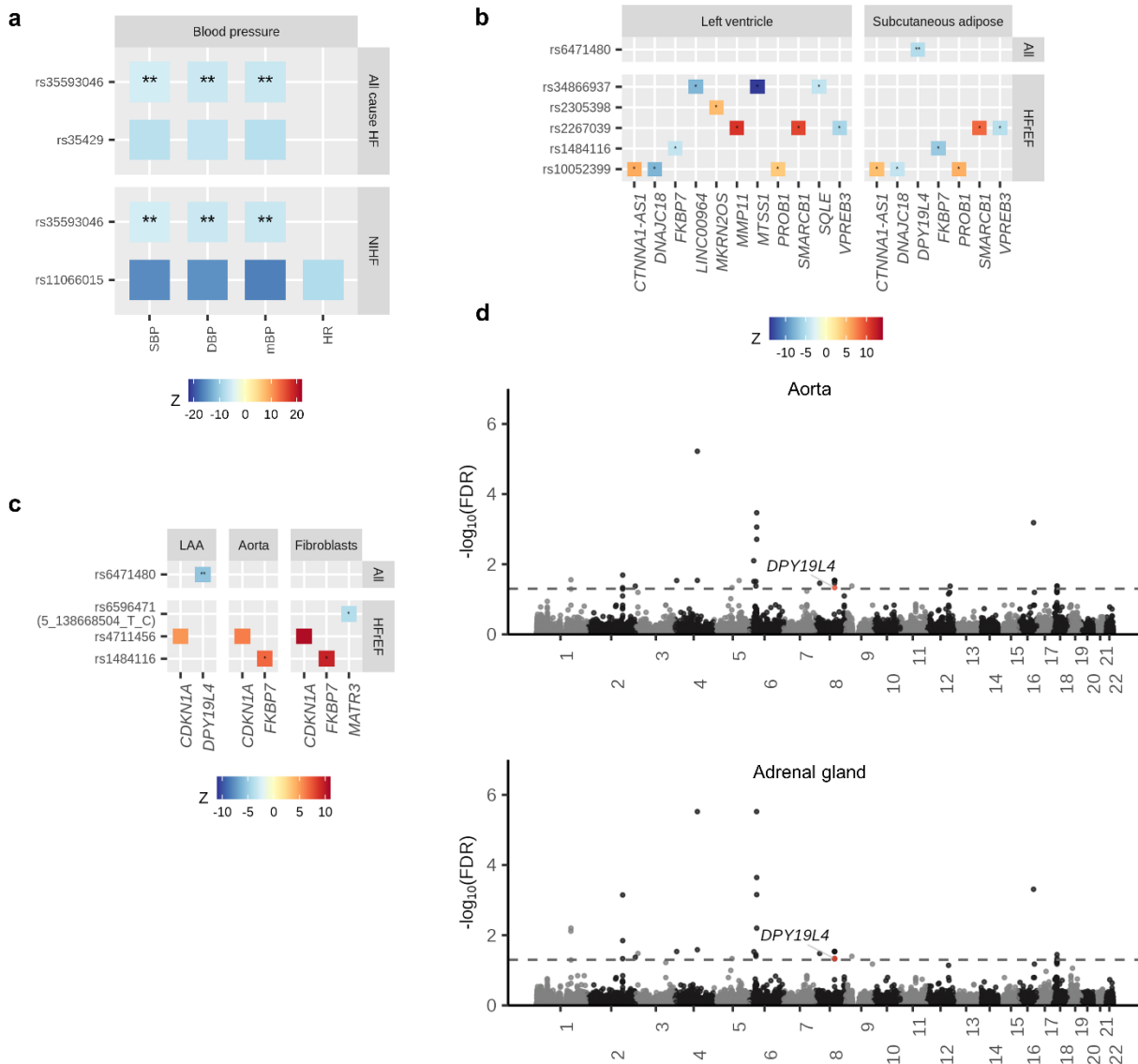
### Supplementary Fig. 3 | Comparison of allelic effects and allelic effects identified in

**Japanese GWAS.** (a and b) Comparison of allelic effects (a) and allele frequency (b) between BBJ 1<sup>st</sup> and BBJ 2<sup>nd</sup>. Effect size with its 95%CI or allele frequency of BBJ 1<sup>st</sup> GWAS are shown in the x-axis, and those of BBJ 2<sup>nd</sup> are shown in the y-axis. (c and d) Comparison of allelic effects (c) and allele frequencies (d) between our Japanese GWAS (BBJ) and European GWAS. Effect size and its 95%CI, or allele frequencies of BBJ are shown in the x-axis, and those of

207 European GWAS are shown in the y-axis. Points are shown in red if new loci and in blue if  
208 previously reported only in MTAG but not in GWAS. CI, confidence interval; GWAS, genome-  
209 wide association study; HF, heart failure; MTAG, multi-trait analysis of GWAS; QQ, quantile-  
210 quantile.

211

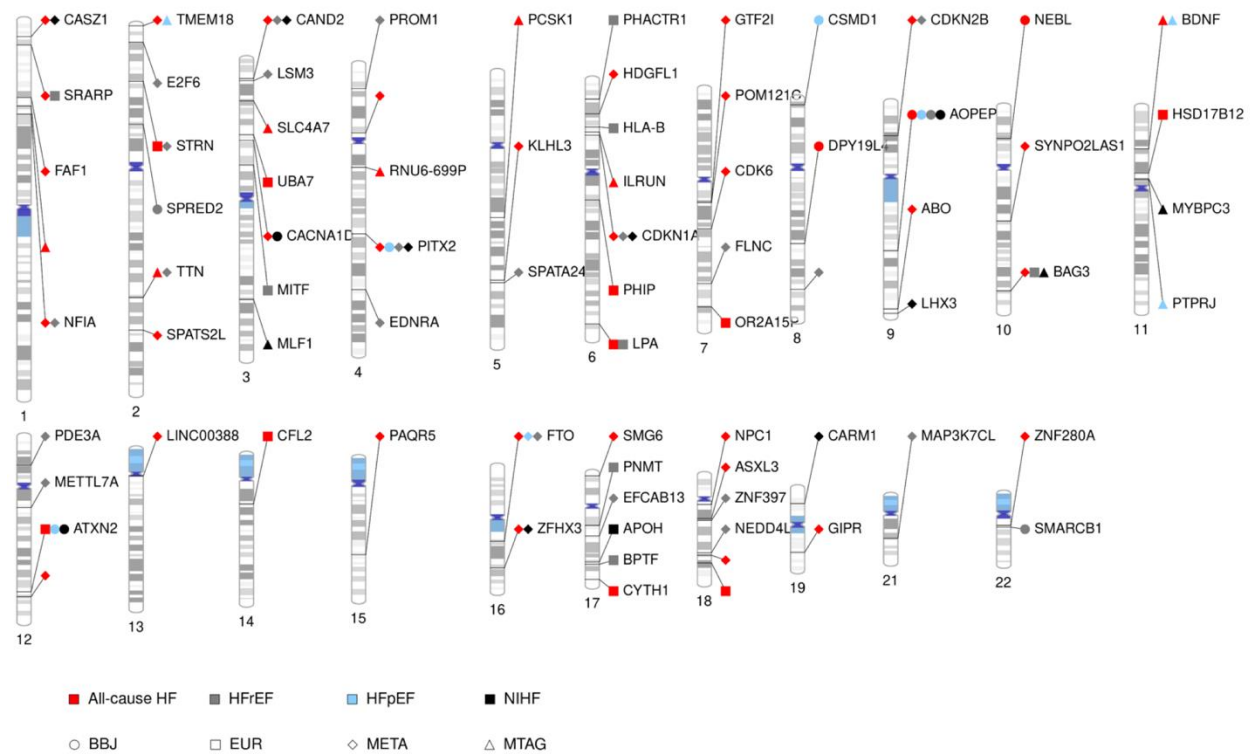




**Supplementary Fig. 4 | Downstream analysis of Japanese GWAS.** (a) Lead variants identified in our Japanese GWAS of each HF phenotype are searched in previously reported Japanese GWAS of cardiovascular-related phenotypes. The color indicates the Z value of the corresponding Japanese GWAS. (b and c) Lead variants identified by each HF phenotype Japanese GWAS are searched in GTEx eQTL (b) and sQTL (c). The color indicates the Z value of the corresponding eQTL or sQTL. rs6596471, which was strongly correlated with lead variant chr5:138668504:T:C ( $r^2 > 0.8$ ) is used as proxy variant since chr5:138668504:T:C was not found

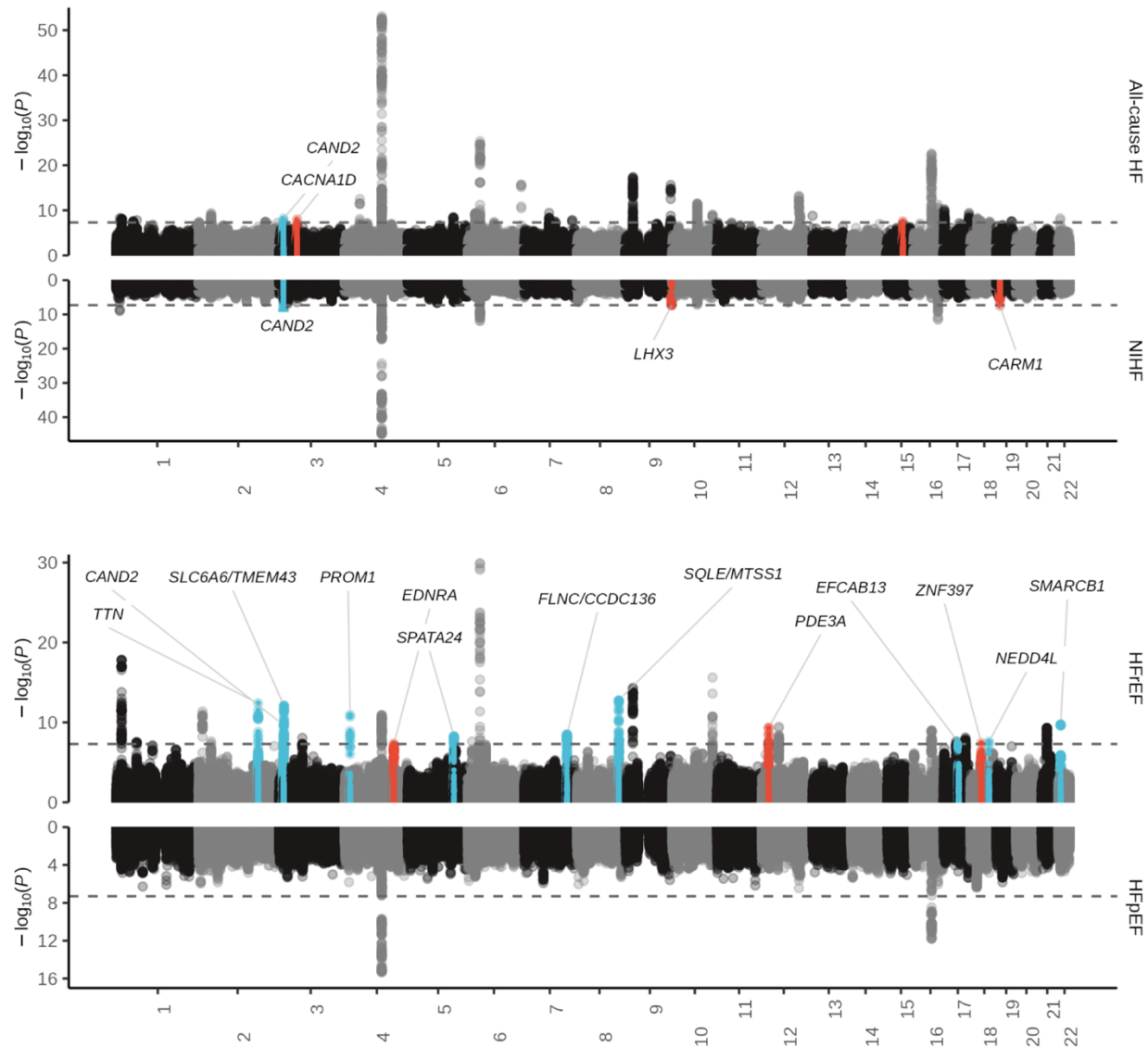
220 in GTEx database. **(d)** Manhattan plots of H-MAGMA using aorta or adrenal gland Hi-C  
 221 datasets.  $-\log_{10}(\text{FDR})$  on the y-axis are shown against the genomic positions (hg19) on the x-axis.  
 222 Genes that have not been identified in previous TWAS, proteome-wide MR, or gene analysis are  
 223 shown in red. \*\* indicates novel loci, and \* indicates loci previously reported only in MTAG and  
 224 not in GWAS. eQTL, expression quantitative trait loci; GWAS, genome-wide association study;  
 225 HF, heart failure; HFpEF, heart failure with preserved ejection fraction; HFrEF, heart failure  
 226 with reduced ejection fraction; H-MAGMA, Hi-C coupled MAGMA; LAA, left atrial  
 227 appendage; MTAG, multi-trait analysis of GWAS; NIHF, non-ischemic heart failure; sQTL,  
 228 splicing quantitative trait loci.

229



## Supplementary Fig. 5 | Phenogram of genome-wide significant loci for HF and its subtypes.

Indicated gene names are the prioritized gene when one gene is prioritized by our methods, the nearest gene when multiple genes are prioritized equally, and the blank when none is prioritized and nearest gene is RNA gene. The shapes indicate HF subtypes; circles, all-cause HF; rectangles, HFrEF; triangles, HFpEF; and diamonds, non-ischemic HF. Colors indicate HF and its subtypes; red, BioBank Japan (BBJ); gray, European (EUR); light green, trans-ancestry meta-analysis (META); and black, multi-trait analysis of GWAS (MTAG). Cytobands and annotations are based on GRCh37/hg19. Gene names were annotated if prioritized by at least 3 methods.



**Supplementary Fig. 6 | Results of the cross-ancestry meta-analysis.** Miami plot of trans-

ancestry meta-analysis.  $-\log_{10}(P)$  value on the y-axis is shown against the genomic positions

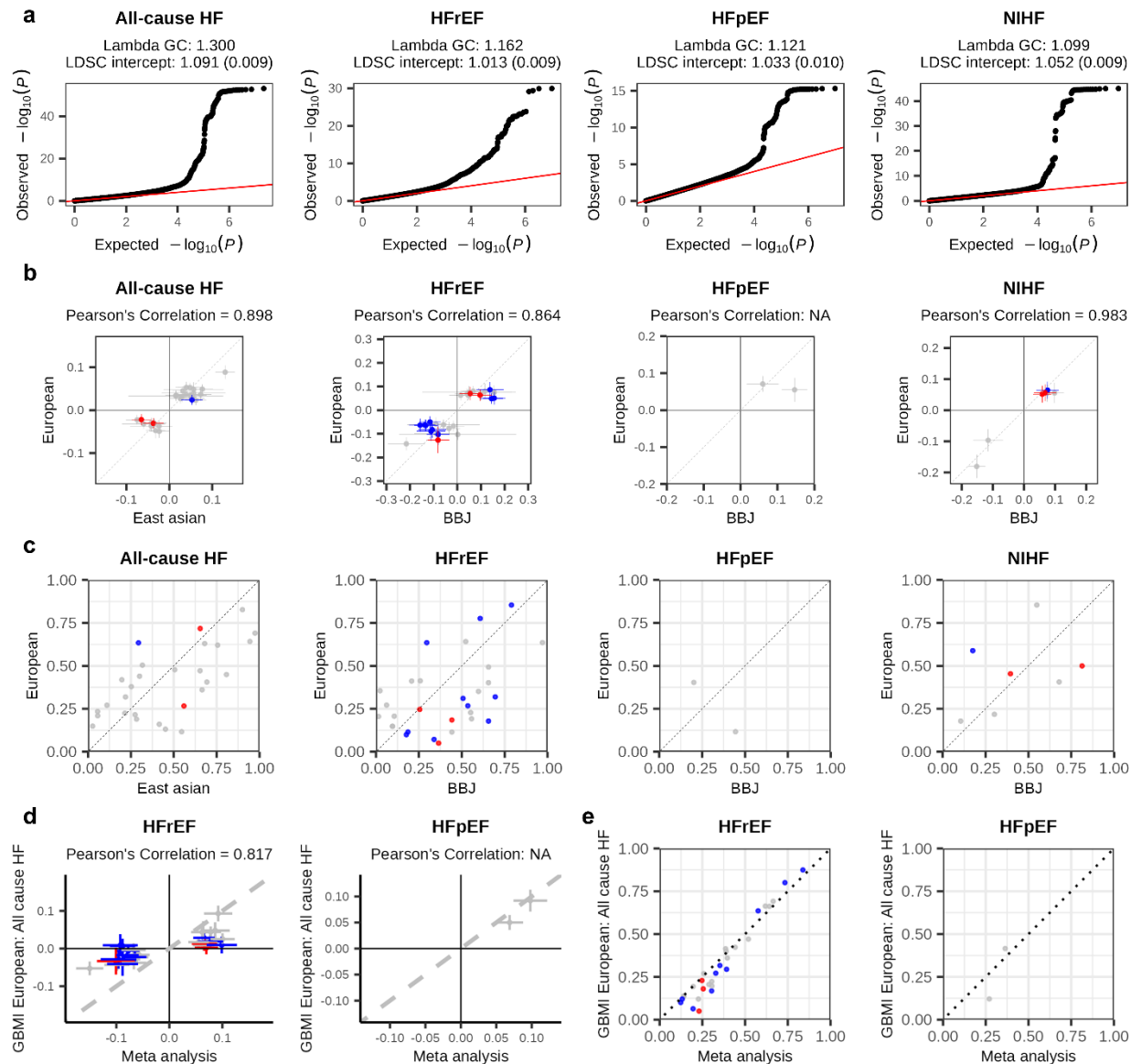
(hg19) on the x-axis. Association signals that reached a genome-wide significance level ( $P < 5 \times$

$10^{-8}$ ) are shown in red if new loci and in blue if previously reported only in MTAG but not in

GWAS. GWAS, genome-wide association study; HF, heart failure; HFrEF, heart failure with

reduced ejection fraction; HFpEF, heart failure with preserved ejection fraction; MTAG, multi-

trait analysis of GWAS.

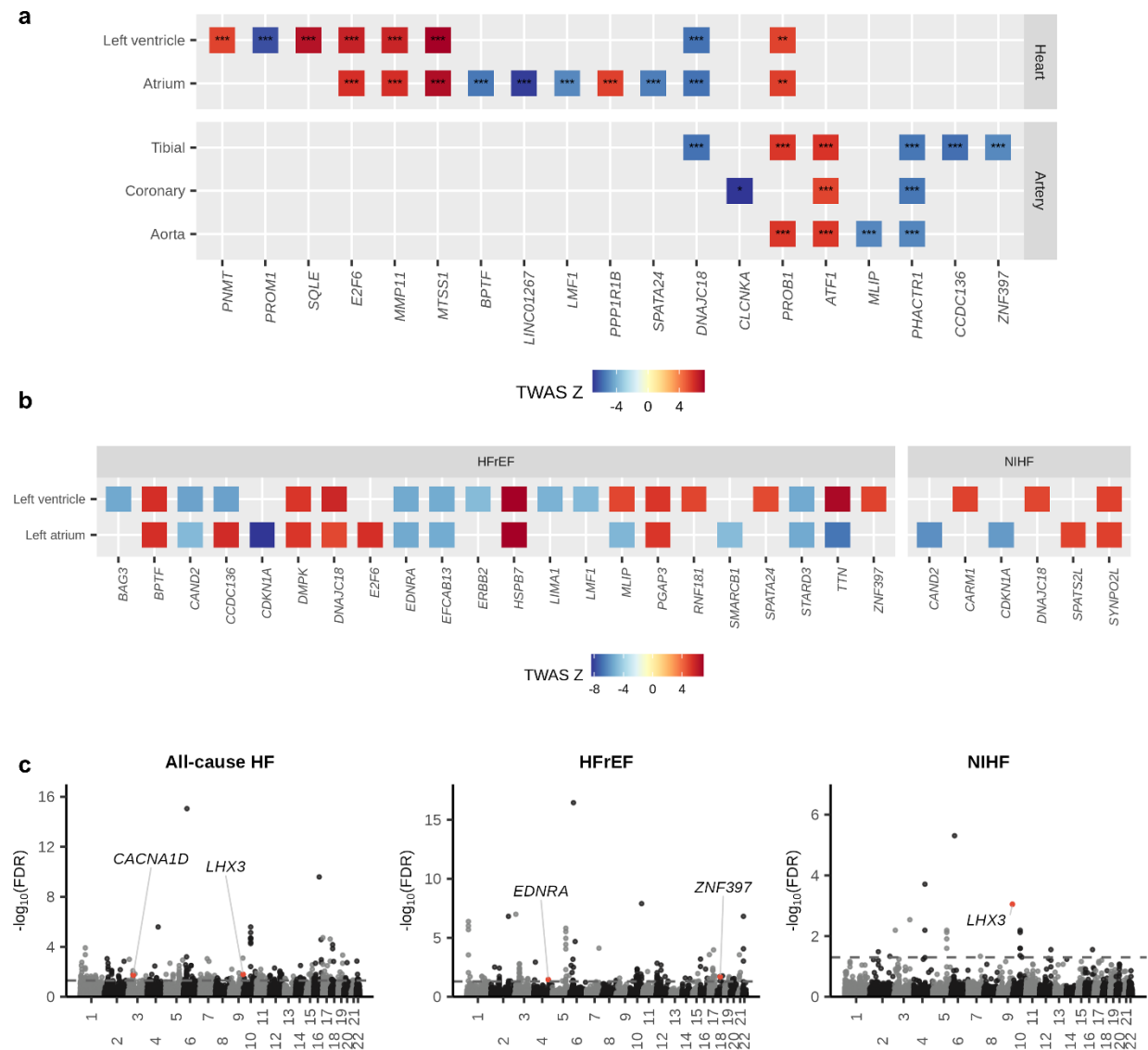


**Supplementary Fig. 7 | QQ plot and comparison of allele frequencies and allelic effects**

**identified in the cross-ancestry meta-analysis. (a)** QQ plot for each HF phenotype in the cross-ancestry meta-analysis. Two-sided  $P$  values were calculated using a logistic regression model. **(b)** and **(c)** Comparison of allelic effects **(b)** and allele frequency **(c)** between East Asian GWAS and European GWAS. Effect size with its 95%CI or allele frequency of East Asian (for all-cause HF) or BBJ (other HF phenotypes) GWAS are shown in the  $x$ -axis, and those of European are shown in the  $y$ -axis. **(d and e)** Comparison of allelic effects between the cross-ancestry meta-analysis

256 (HFrEF or HFpEF) and non-overlapping European GWAS (GBMI European all-cause HF).  
 257 Effect size with its 95%CI (**d**) or allele frequencies (**e**) of the cross-ancestry meta-analysis are  
 258 shown in the *x*-axis, and those of European GWAS are shown in the *y*-axis. Points are shown in  
 259 red if new loci and in blue if previously reported only in MTAG but not in GWAS. CI,  
 260 confidence interval; GWAS, genome-wide association study; HF, heart failure; HFrEF, heart  
 261 failure with reduced ejection fraction; HFpEF, heart failure with preserved ejection fraction;  
 262 MTAG, multi-trait analysis of GWAS; QQ, quantile-quantile.

263

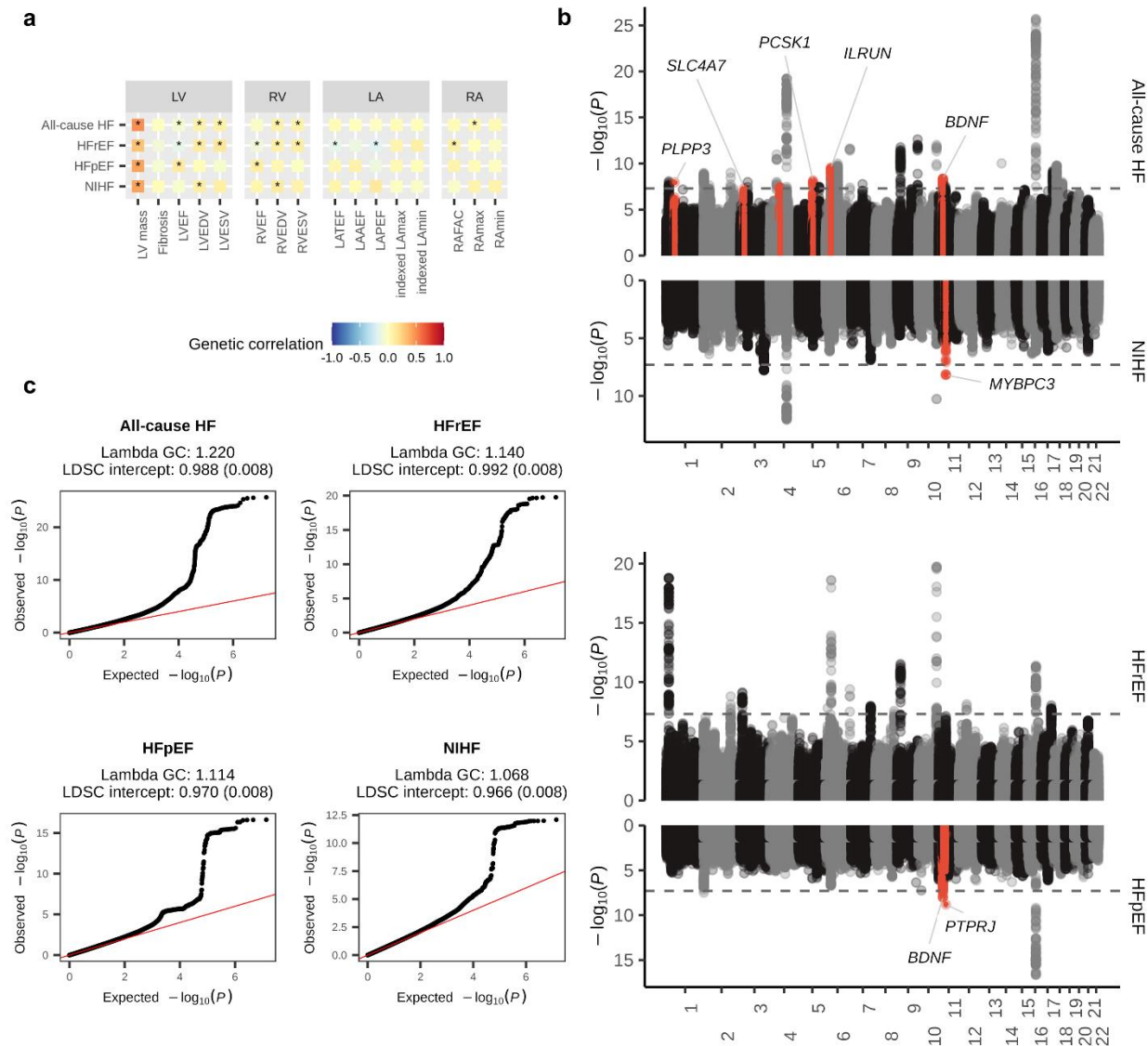


**Supplementary Fig. 8 | Downstream analysis of the cross-ancestry meta-analysis. (a)**

Heatmap of the TWAS of HF (all-cause HF and HF subtypes) showing transcriptome-wide significant associations with supporting evidence from colocalization. Colored squares TWAS significant associations based on two-sided  $P$  values after multiple testing corrections ( $P < 1.55 \times 10^{-6}$ ). \* indicate PP4 0.75-0.8, \*\* 0.8-0.9, \*\*\* 0.9-1.0. (b) Heatmap of the Splicing-TWAS HF showing splicing-wide significant associations. Colored squares splicing-TWAS significant associations based on two-sided  $P$  values after multiple testing corrections. Genes are

presented on the  $x$ -axis, and tissue types are on the  $y$ -axis in both **(a)** and **(b)**. **(c)** Manhattan plots of MAGMA for all-cause HF, HFrEF, and non-ischemic heart failure.  $-\log_{10}(\text{FDR})$  on the  $y$ -axis are shown against the genomic positions (hg19) on the  $x$ -axis. Genes that have not been identified in previous TWAS, proteome-wide MR, or gene analysis are shown in red. HF, heart failure; TWAS, transcriptome-wide association studies.



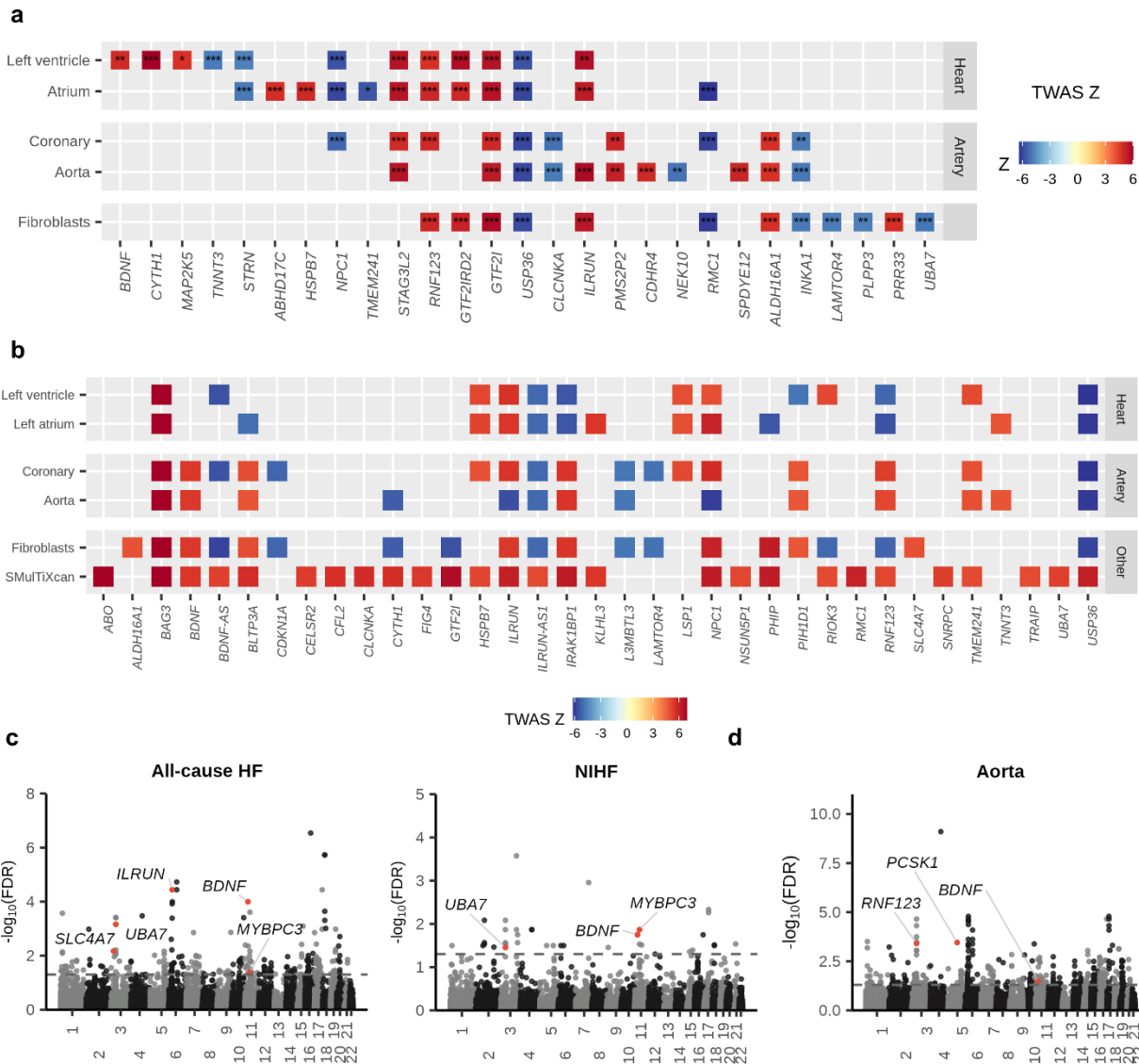


**Supplementary Fig. 9 | Results of multi-trait analysis of GWAS. (a) Genetic correlation**

between HF and cardiac MRI-derived parameters. Significant genetic correlations ( $P < 0.05$ ) are marked with an asterisk. Two-sided  $P$  values were calculated using linkage disequilibrium score regression. (b) Miami plot of MTAG.  $-\log_{10}(P)$  value) on the y-axis are shown against the genomic positions (hg19) on the x-axis. Association signals that reached a genome-wide significance level ( $P < 5 \times 10^{-8}$ ) are shown in red if new loci. (c) QQ plot for each HF phenotype in MTAG. GWAS, genome-wide association study; HF, heart failure; HFpEF, heart failure with

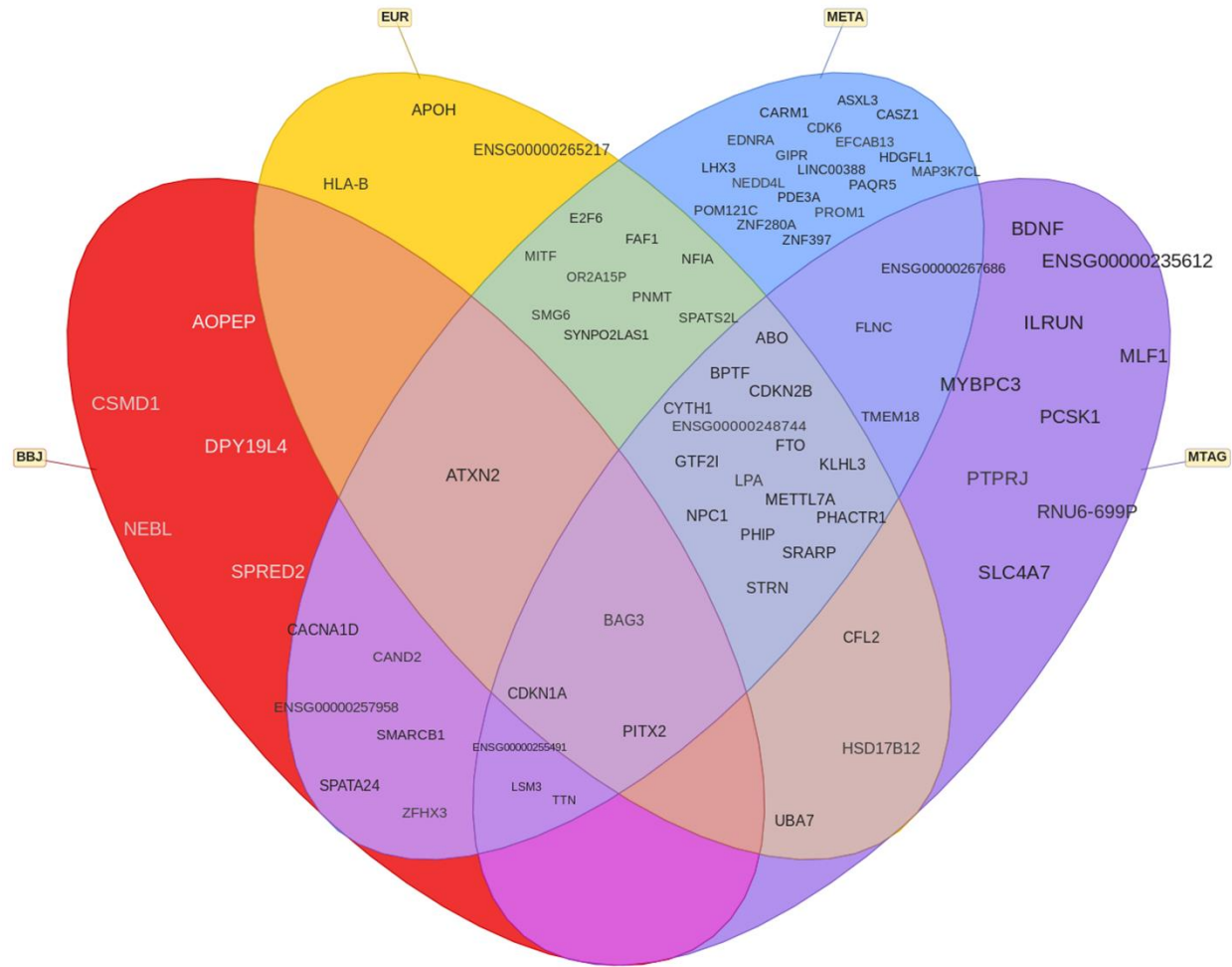
286 preserved ejection fraction; HFrEF, heart failure with reduced ejection fraction; MTAG, multi-  
287 trait analysis of GWAS; NIHF, non-ischemic heart failure; QQ, quantile-quantile.

288

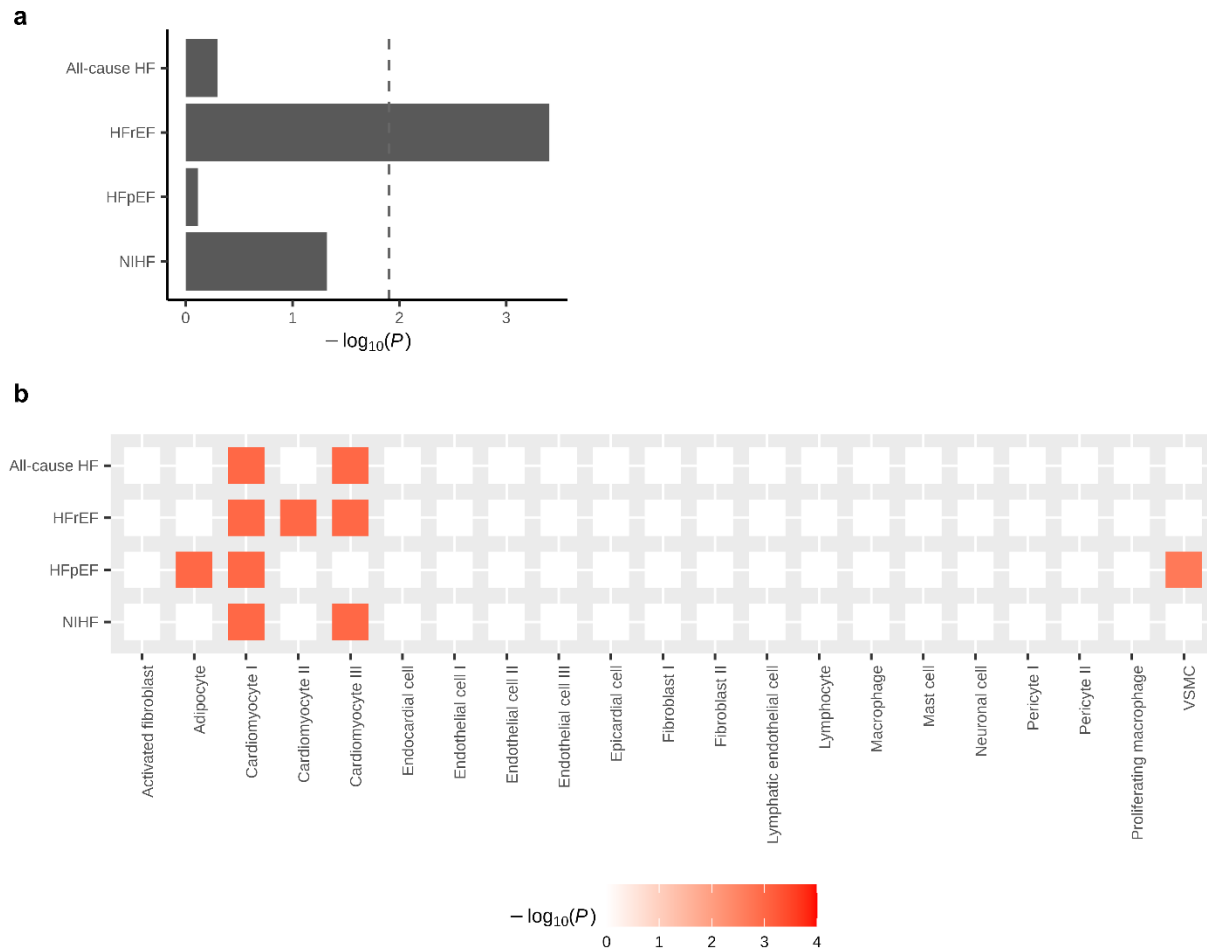


**Supplementary Fig. 10 | Downstream analysis of multi-trait analysis of GWAS. (a)** Heatmap of the TWAS showing transcriptome-wide significant associations with supporting evidence from colocalization. Colored squares TWAS significant associations based on two-sided  $P$  values after multiple testing corrections ( $P < 1.55 \times 10^{-6}$ ). \* indicate PP4 0.75-0.8, \*\* 0.8-0.9, \*\*\* 0.9-1.0. **(b)** Heatmap of the Splicing-TWAS HF showing splicing-wide significant associations. Colored squares splicing-TWAS significant associations based on two-sided  $P$  values after multiple testing corrections. Genes are presented on the  $x$ -axis, and tissue types are

297 on the  $y$ -axis in both **(a)** and **(b)**. **(c and d)** Manhattan plots of MAGMA for all-cause HF or non-  
298 ischemic heart failure **(c)**, and H-MAGMA using aorta Hi-C datasets in all-cause HF**(d)**. -  
299  $\log_{10}(\text{FDR})$  on the  $y$ -axis are shown against the genomic positions (hg19) on the  $x$ -axis. Genes  
300 that have not been identified in previous TWAS, proteome-wide MR, or gene analysis are shown  
301 in red. HF, heart failure; TWAS, transcriptome-wide association studies.  
302

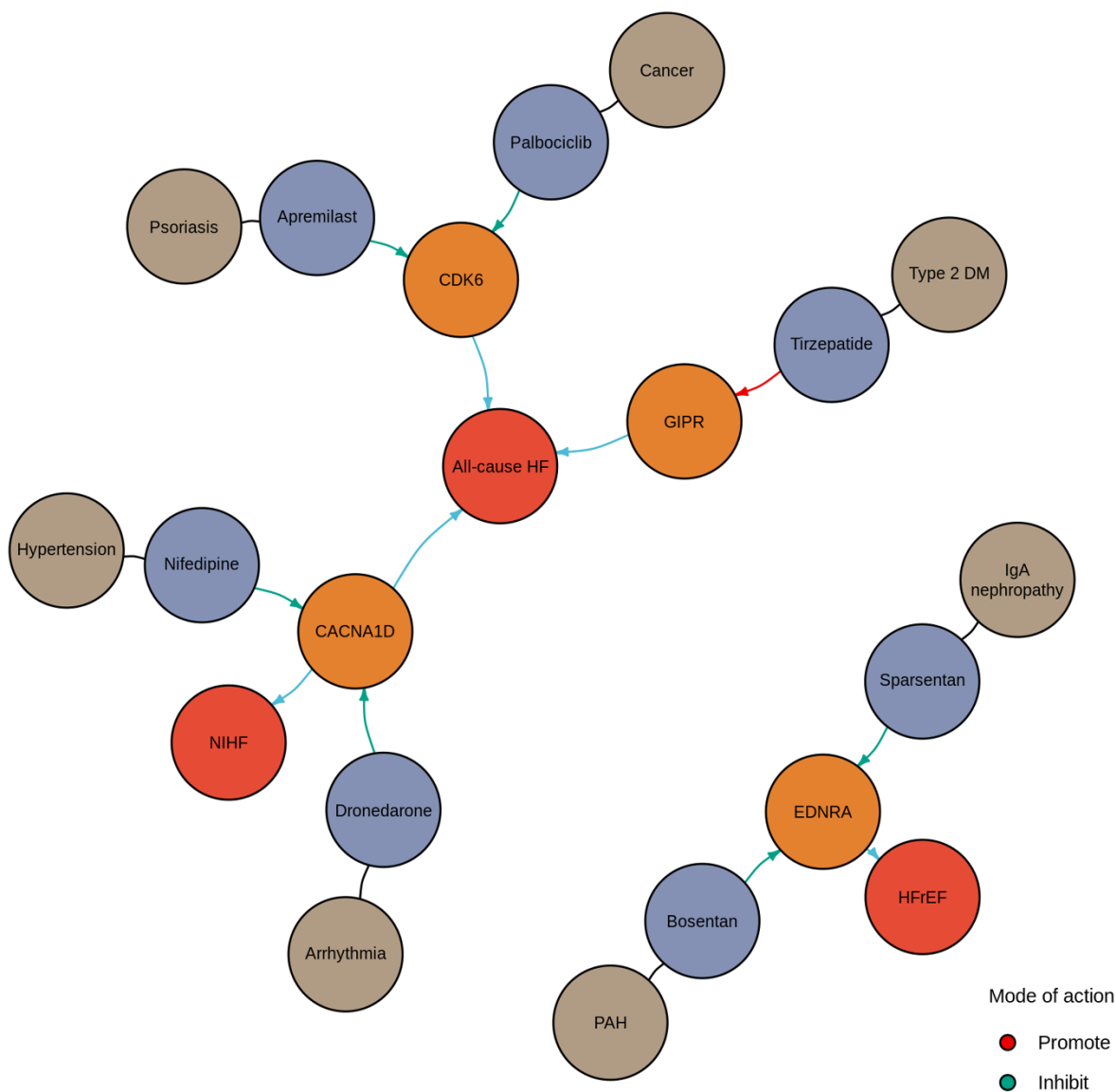


**Supplementary Fig. 11 | Benn diagram for genes identified by each analysis.** BBJ, BioBank Japan; EUR, European; META, meta-analysis; MTAG, multi-trait analysis of GWAS.

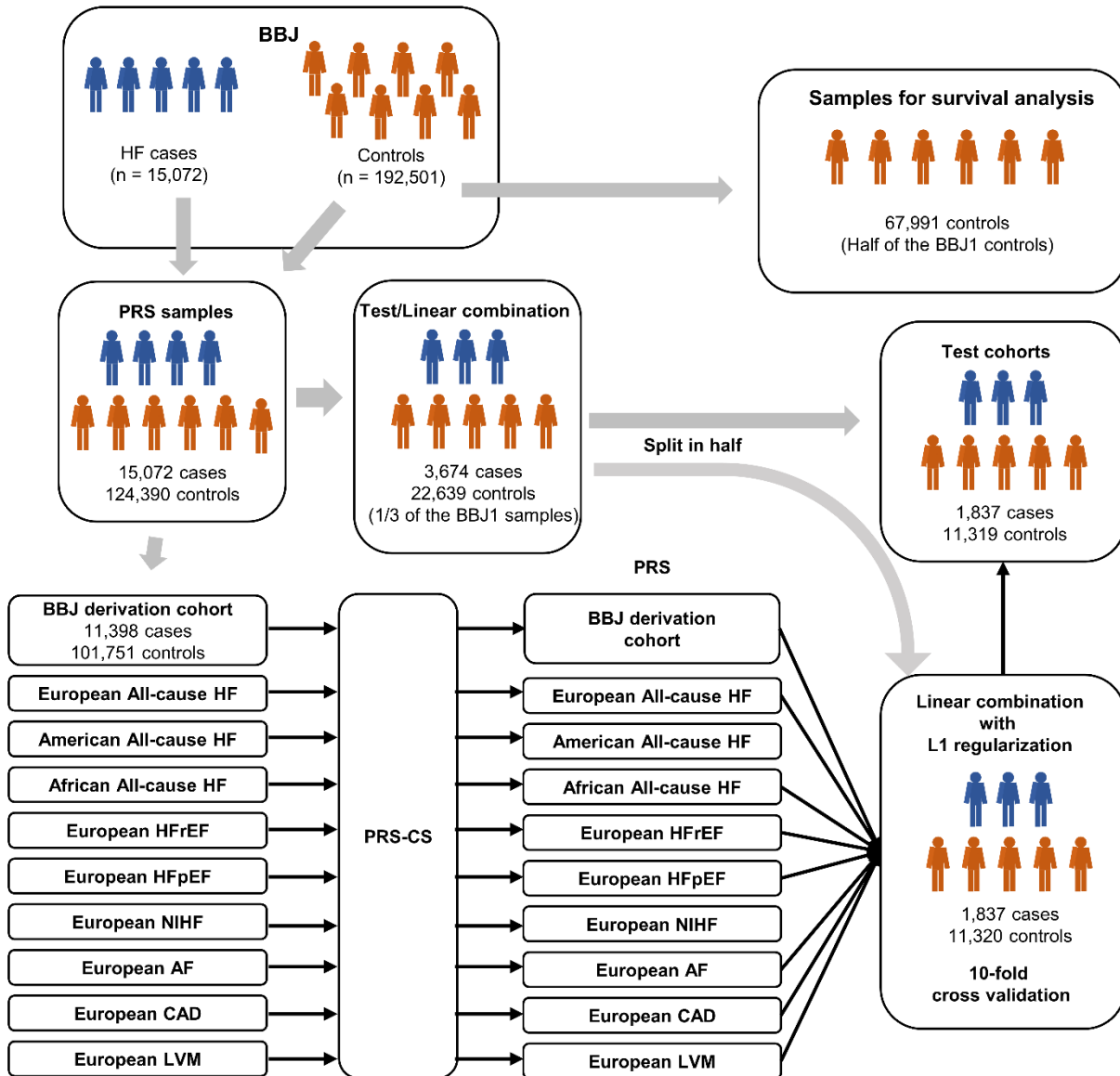


## Supplementary Fig. 12 | miRNA enrichment analysis and single-cell enrichment analysis.

(a) MIGWAS results of the four HF phenotypes. The overall contribution of miRNA-target gene network to the traits through the tissue-naïve approach. An enrichment signal is shown by  $-\log_{10}(P_{\text{MIGWAS}})$ . (b) Heatmaps depicting each cell type-disease association for HF phenotypes. Heatmap colors denote uncorrected  $P$  value of cell-type-disease association evaluated using scDRS. Only significant associations are shown.

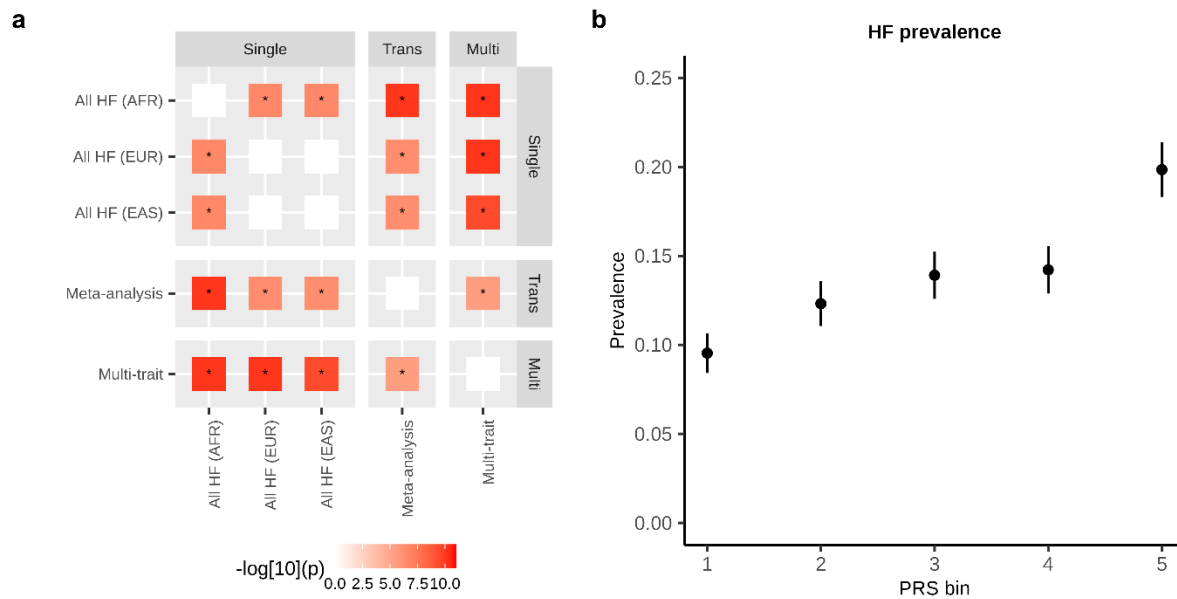


**Supplementary Fig. 13 | Candidate drugs linked to disease susceptibility loci for HF.** Dark blue indicates HF subtypes; orange gene; purple medications; and brown diseases.



**Supplementary Fig. 14 | Analytical scheme for PRS development.** Schematic representation for derivation, cross-validation, performance testing of HF-PRS in the independent test cohort, and survival analysis for HF-PRS.





**Supplementary Fig. 15 | PRS performance. (a)** Pairwise comparison of PRS performance.

Distribution of the pairwise difference of Nagelkerke's pseudo- $R^2$  ( $\Delta$  pseudo- $R^2$ : Pseudo  $R^2_{\text{Score}}$

$Y - \text{Pseudo } R^2_{\text{Score}} X$ ,  $X$ , and  $Y$  are found at the axis) between each pair of PRS models. The

distributions were obtained by bootstrapping  $5.0 \times 10^4$  times. Two-sided bootstrap  $P$  values were

calculated by counting the number of  $\Delta$  pseudo- $R^2 \leq 0$  or  $\Delta$  pseudo- $R^2 > 0$  and then multiplying

the lower value by the minimum estimated  $P$  value ( $2 * 1 / (5.0 \times 10^4) = 4 \times 10^{-5}$ : two-sided).

The significance was set at  $P = 5.0 \times 10^{-3}$  (0.05/10). **(b)** PRS distribution and HF prevalence.

Prevalence of HF based on the HF-PRS deciles in each combination of GWAS. The number of

individuals in each decile is 2,631-2,632. Data are presented as medians and 95% CI. PRS,

polygenic risk score; CI, confidence interval.

## Members of participating consortia

### The Biobank Japan Project

Koichi Matsuda<sup>1,2</sup>, Takayuki Morisaki<sup>2,3</sup>, Yukinori Okada<sup>4</sup>, Yoichiro Kamatani<sup>5</sup>, Kaori Muto<sup>6</sup>, Akiko Nagai<sup>6</sup>, Yoji Sagiya<sup>2</sup>, Natsuhiko Kumasaka<sup>7</sup>, Yoichi Furukawa<sup>8</sup>, Yuji Yamanashi<sup>3</sup>, Yoshinori Murakami<sup>3</sup>, Yusuke Nakamura<sup>3</sup>, Wataru Obara<sup>9</sup>, Ken Yamaji<sup>10</sup>, Kazuhisa Takahashi<sup>11</sup>, Satoshi Asai<sup>12,13</sup>, Yasuo Takahashi<sup>13</sup>, Shinichi Higashiue<sup>14</sup>, Shuzo Kobayashi<sup>14</sup>, Hiroki Yamaguchi<sup>15</sup>, Yasunobu Nagata<sup>15</sup>, Satoshi Wakita<sup>15</sup>, Chikako Nito<sup>16</sup>, Yu-ki Iwasaki<sup>17</sup>, Shigeo Murayama<sup>18</sup>, Kozo Yoshimori<sup>19</sup>, Yoshio Miki<sup>20</sup>, Daisuke Obata<sup>21</sup>, Masahiko Higashiyama<sup>22</sup>, Akihide Masumoto<sup>23</sup>, Yoshinobu Koga<sup>23</sup> & Yukihiro Koretsune<sup>24</sup>

<sup>1</sup>Laboratory of Genome Technology, Human Genome Center, Institute of Medical Science, The University of Tokyo, Tokyo, Japan.

<sup>2</sup>Laboratory of Clinical Genome Sequencing, Graduate School of Frontier Sciences, The University of Tokyo, Tokyo, Japan.

<sup>3</sup>The Institute of Medical Science, The University of Tokyo, Tokyo, Japan.

<sup>4</sup>Department of Genome Informatics, Graduate School of Medicine, The University of Tokyo, Tokyo, Japan.

<sup>5</sup>Laboratory of Complex Trait Genomics, Graduate School of Frontier Sciences, The University of Tokyo, Tokyo, Japan.

<sup>6</sup>Department of Public Policy, Institute of Medical Science, The University of Tokyo, Tokyo, Japan.

<sup>7</sup>Division of Digital Genomics, Institute of Medical Science, The University of Tokyo, Tokyo, Japan.

<sup>8</sup> Division of Clinical Genome Research, Institute of Medical Science, The University of Tokyo, Tokyo, Japan.

<sup>9</sup> Department of Urology, Iwate Medical University, Iwate, Japan.

<sup>10</sup> Department of Internal Medicine and Rheumatology, Juntendo University Graduate School of Medicine, Tokyo, Japan.

<sup>11</sup> Department of Respiratory Medicine, Juntendo University Graduate School of Medicine, Tokyo, Japan.

<sup>12</sup> Division of Pharmacology, Department of Biomedical Science, Nihon University School of Medicine, Tokyo, Japan.

<sup>13</sup> Division of Genomic Epidemiology and Clinical Trials, Clinical Trials Research Center, Nihon University. School of Medicine, Tokyo, Japan.

<sup>14</sup> Tokushukai Group, Tokyo, Japan.

<sup>15</sup> Department of Hematology, Nippon Medical School, Tokyo, Japan.

<sup>16</sup> Laboratory for Clinical Research, Collaborative Research Center, Nippon Medical School, Tokyo, Japan.

<sup>17</sup> Department of Cardiovascular Medicine, Nippon Medical School, Tokyo, Japan.

<sup>18</sup> Tokyo Metropolitan Geriatric Hospital and Institute of Gerontology, Tokyo, Japan.

<sup>19</sup> Fukujuji Hospital, Japan Anti-Tuberculosis Association, Tokyo, Japan.

<sup>20</sup> The Cancer Institute Hospital of the Japanese Foundation for Cancer Research, Tokyo, Japan.

<sup>21</sup> Center for Clinical Research and Advanced Medicine, Shiga University of Medical Science, Shiga, Japan.

<sup>22</sup> Department of General Thoracic Surgery, Osaka International Cancer Institute, Osaka, Japan.

<sup>23</sup> Iizuka Hospital, Fukuoka, Japan.

381      <sup>24</sup> National Hospital Organization Osaka National Hospital, Osaka, Japan.

382

## References

1. Levin MG, Tsao NL, Singhal P, Liu C, Vy HMT, Paranjpe I, Backman JD, Bellomo TR, Bone WP, Biddinger KJ, Hui Q, Dikilitas O, Satterfield BA, Yang Y, Morley MP, Bradford Y, Burke M, Reza N, Charest B, Regeneron Genetics C, Judy RL, Puckelwartz MJ, Hakonarson H, Khan A, Kottyan LC, Kullo I, Luo Y, McNally EM, Rasmussen-Torvik LJ, Day SM, Do R, Phillips LS, Ellinor PT, Nadkarni GN, Ritchie MD, Arany Z, Cappola TP, Margulies KB, Aragam KG, Haggerty CM, Joseph J, Sun YV, Voight BF and Damrauer SM. Genome-wide association and multi-trait analyses characterize the common genetic architecture of heart failure. *Nat Commun.* 2022;13:6914.
2. Joseph J, Liu C, Hui Q, Aragam K, Wang Z, Charest B, Huffman JE, Keaton JM, Edwards TL, Demissie S, Djousse L, Casas JP, Gaziano JM, Cho K, Wilson PWF, Phillips LS, Program VAMV, O'Donnell CJ and Sun YV. Genetic architecture of heart failure with preserved versus reduced ejection fraction. *Nat Commun.* 2022;13:7753.
3. Aragam KG, Chaffin M, Levinson RT, McDermott G, Choi SH, Shoemaker MB, Haas ME, Weng LC, Lindsay ME, Smith JG, Newton-Cheh C, Roden DM, London B, Investigators G, Wells QS, Ellinor PT, Kathiresan S, Lubitz SA and Genetic Risk Assessment of Defibrillator Events I. Phenotypic Refinement of Heart Failure in a National Biobank Facilitates Genetic Discovery. *Circulation.* 2019;139:489-501.
4. Pei YF, Liu YZ, Yang XL, Zhang H, Feng GJ, Wei XT and Zhang L. The genetic architecture of appendicular lean mass characterized by association analysis in the UK Biobank study. *Commun Biol.* 2020;3:608.

- 404 5. Zhang L, Bartz TM, Santanasto A, Djousse L, Mukamal KJ, Forman DE, Hirsch CH,  
405 Newman AB, Gottdiener JS and Kizer JR. Body Composition and Incident Heart Failure in  
406 Older Adults: Results From 2 Prospective Cohorts. *J Am Heart Assoc.* 2022;11:e023707.
- 407 6. Gu Q, Yazdanpanah M, van Hoek M, Hofman A, Gao X, de Rooij FW and Sijbrands EJ.  
408 Common variants in PCSK1 influence blood pressure and body mass index. *J Hum Hypertens.*  
409 2015;29:82-6.
- 410 7. Donertas HM, Fabian DK, Valenzuela MF, Partridge L and Thornton JM. Common  
411 genetic associations between age-related diseases. *Nat Aging.* 2021;1:400-412.
- 412 8. Koyama S, Ito K, Terao C, Akiyama M, Horikoshi M, Momozawa Y, Matsunaga H, Ieki  
413 H, Ozaki K, Onouchi Y, Takahashi A, Nomura S, Morita H, Akazawa H, Kim C, Seo JS, Higasa  
414 K, Iwasaki M, Yamaji T, Sawada N, Tsugane S, Koyama T, Ikezaki H, Takashima N, Tanaka K,  
415 Arisawa K, Kuriki K, Naito M, Wakai K, Suna S, Sakata Y, Sato H, Hori M, Sakata Y, Matsuda  
416 K, Murakami Y, Aburatani H, Kubo M, Matsuda F, Kamatani Y and Komuro I. Population-  
417 specific and trans-ancestry genome-wide analyses identify distinct and shared genetic risk loci  
418 for coronary artery disease. *Nat Genet.* 2020;52:1169-1177.
- 419 9. Vuckovic D, Bao EL, Akbari P, Lareau CA, Mousas A, Jiang T, Chen MH, Raffield LM,  
420 Tardaguila M, Huffman JE, Ritchie SC, Megy K, Ponstingl H, Penkett CJ, Albers PK, Wigdor  
421 EM, Sakaue S, Moscati A, Manansala R, Lo KS, Qian H, Akiyama M, Bartz TM, Ben-Shlomo  
422 Y, Beswick A, Bork-Jensen J, Bottinger EP, Brody JA, van Rooij FJA, Chitrala KN, Wilson  
423 PWF, Choquet H, Danesh J, Di Angelantonio E, Dimou N, Ding J, Elliott P, Esko T, Evans MK,  
424 Felix SB, Floyd JS, Broer L, Grarup N, Guo MH, Guo Q, Greinacher A, Haessler J, Hansen T,  
425 Howson JMM, Huang W, Jorgenson E, Kacprowski T, Kahonen M, Kamatani Y, Kanai M,  
426 Karthikeyan S, Koskeridis F, Lange LA, Lehtimäki T, Linneberg A, Liu Y, Lyytikäinen LP,

427 Manichaikul A, Matsuda K, Mohlke KL, Mononen N, Murakami Y, Nadkarni GN, Nikus K,  
 428 Pankratz N, Pedersen O, Preuss M, Psaty BM, Raitakari OT, Rich SS, Rodriguez BAT, Rosen  
 429 JD, Rotter JI, Schubert P, Spracklen CN, Surendran P, Tang H, Tardif JC, Ghanbari M, Volker  
 430 U, Volzke H, Watkins NA, Weiss S, Program VAMV, Cai N, Kundu K, Watt SB, Walter K,  
 431 Zonderman AB, Cho K, Li Y, Loos RJJ, Knight JC, Georges M, Stegle O, Evangelou E, Okada  
 432 Y, Roberts DJ, Inouye M, Johnson AD, Auer PL, Astle WJ, Reiner AP, Butterworth AS,  
 433 Ouwehand WH, Lettre G, Sankaran VG and Soranzo N. The Polygenic and Monogenic Basis of  
 434 Blood Traits and Diseases. *Cell*. 2020;182:1214-1231 e11.

435 10. Astle WJ, Elding H, Jiang T, Allen D, Ruklisa D, Mann AL, Mead D, Bouman H,  
 436 Riveros-Mckay F, Kostadima MA, Lambourne JJ, Sivapalaratnam S, Downes K, Kundu K,  
 437 Bombá L, Berentsen K, Bradley JR, Daugherty LC, Delaneau O, Freson K, Garner SF, Grassi L,  
 438 Guerrero J, Haimel M, Janssen-Megens EM, Kaan A, Kamat M, Kim B, Mandoli A, Marchini J,  
 439 Martens JHA, Meacham S, Megy K, O'Connell J, Petersen R, Sharifi N, Sheard SM, Staley JR,  
 440 Tuna S, van der Ent M, Walter K, Wang SY, Wheeler E, Wilder SP, Iotchkova V, Moore C,  
 441 Sambrook J, Stunnenberg HG, Di Angelantonio E, Kaptoge S, Kuipers TW, Carrillo-de-Santa-  
 442 Pau E, Juan D, Rico D, Valencia A, Chen L, Ge B, Vasquez L, Kwan T, Garrido-Martin D, Watt  
 443 S, Yang Y, Guigo R, Beck S, Paul DS, Pastinen T, Bujold D, Bourque G, Frontini M, Danesh J,  
 444 Roberts DJ, Ouwehand WH, Butterworth AS and Soranzo N. The Allelic Landscape of Human  
 445 Blood Cell Trait Variation and Links to Common Complex Disease. *Cell*. 2016;167:1415-1429  
 446 e19.

447 11. Finucane HK, Reshef YA, Anttila V, Slowikowski K, Gusev A, Byrnes A, Gazal S, Loh  
 448 PR, Lareau C, Shores N, Genovese G, Saunders A, Macosko E, Pollack S, Brainstorm C, Perry  
 449 JRB, Buenrostro JD, Bernstein BE, Raychaudhuri S, McCarroll S, Neale BM and Price AL.

450 Heritability enrichment of specifically expressed genes identifies disease-relevant tissues and cell  
451 types. *Nat Genet.* 2018;50:621-629.

452 12. Sakaue S, Hirata J, Maeda Y, Kawakami E, Nii T, Kishikawa T, Ishigaki K, Terao C,  
453 Suzuki K, Akiyama M, Suita N, Masuda T, Ogawa K, Yamamoto K, Saeki Y, Matsushita M,  
454 Yoshimura M, Matsuoka H, Ikari K, Taniguchi A, Yamanaka H, Kawaji H, Lassmann T, Itoh M,  
455 Yoshitomi H, Ito H, Ohmura K, AR RF, Hayashizaki Y, Carninci P, Kumanogoh A, Kamatani  
456 Y, de Hoon M, Yamamoto K and Okada Y. Integration of genetics and miRNA-target gene  
457 network identified disease biology implicated in tissue specificity. *Nucleic Acids Res.*  
458 2018;46:11898-11909.

459 13. Zhang MJ, Hou K, Dey KK, Sakaue S, Jagadeesh KA, Weinand K, Taychameekiatchai  
460 A, Rao P, Pisco AO, Zou J, Wang B, Gandal M, Raychaudhuri S, Pasaniuc B and Price AL.  
461 Polygenic enrichment distinguishes disease associations of individual cells in single-cell RNA-  
462 seq data. *Nat Genet.* 2022;54:1572-1580.

463 14. de Leeuw CA, Mooij JM, Heskes T and Posthuma D. MAGMA: generalized gene-set  
464 analysis of GWAS data. *PLoS Comput Biol.* 2015;11:e1004219.  
465